Department of Biomedical Sciences

University of Veterinary Medicine Vienna

Institute of Animal Breeding and Genetics

Head: O.Univ.-Prof. Dr.med.vet. Mathias Müller

# Deciphering the role of STAT1 signaling in myeloid cells in extramedullary erythropoiesis and megakaryopoiesis during murine cytomegalovirus (MCMV) infection

Master Thesis

University of Veterinary Medicine Vienna

Submitted by

Svetlana Pahernik

Vienna, August 2022

Supervisors: Dr[in] Tanja Bulat

Mag[a] rer.nat. Dr[in] rer.nat. Birgit Strobl

## Acknowledgements

First and foremost, I would like to express my deepest gratitude to my supervisors Dr. Tanja Bulat and Dr. Birgit Strobl. I will always be grateful for the time and effort they invested in me, their guidance and valuable lessons. They both inspire me.

I would like to thank Tanja for choosing me to work with her, for sharing her knowledge and expertise with me, for her support during long days of experiments and for answering my every question. The past year has been an unforgettable experience. I also promise to carry on with “the tradition” (she knows what this is about).

I want to thank the head of the Institute of Animal Breeding and Genetics, Univ.-Prof. Dr. Mathias Müller, for giving me the opportunity to work at the institute and for his insightful feedback on my presentations. I am particularly grateful to Dr. Caroline Lassnig and the KA staff members for performing all the *in vivo* experiments.

I would also like to extend my thanks to Jelena Josipović and Lena Amenitsch for their technical support during my experiments.

I thank Kristina Schmidhofer for all the times we cried together (of laughter). I am happy to have shared the experience of joining a lab as a master's student with her. Thanks to all the PhD students (Kathi, Sara, MJ, Lara, Elif, Hrönn, Maria and Andy) for fun times at game nights and dinners.

Because of you all, I always came to the institute with a smile.

I wish to thank my partner Aleks for taking this leap of faith and moving to Vienna with me. His support means everything! Last, but never least, I thank my parents. They truly are ‘my twin pillars without whom I could not stand’.

## Table of Contents

# 1. Introduction

## 1.1 Medullary haematopoiesis

Haematopoiesis is the process in which cellular components of the blood are formed from multipotent hematopoietic stem cells (HSCs) and, in adults, primarily occurrs in the bone marrow. The functionality of HSCs is defined by their capacity to self-renew and their potential to differentiate into all mature blood cell lineages. The recently revised haematopoietic hierarchy proposes the existence of three distinct HSC subpopulations: long-term haematopoietic stem cells (LT-HSC), intermediate-term HSCs (IT-HSC) and short-term HSC (ST-HSC) (Fig. 1) (Zhang et al. 2018). Downstream of HSC is a group of multipotent progenitors (MPP), which are non-self-renewing and can be subdivided into five populations (MPP1-5) (Fig. 1) (Pietras et al. 2015, Sommerkamp et al. 2021). MPP1 can reconstitute multiple cell lineages and are phenotypically similar to ST-HSC (Zhang et al. 2018). MPP2 generate the bipotent common myeloid progenitor (CMP), which then undergoes a bifurcation into the granulocyte/macrophage progenitor (GMP) and megakaryocyte/erythrocyte progenitor (MEP) (Akashi et al. 2000). There is recent evidence that MPP2 are biased towards the megakaryocyte lineage and have the ability to differentiate into megakaryocytes (MK) by bypassing the CMP and MEP stages (Rodriguez-Fraticelli et al. 2018). MPP3 develop into CMP, with a tendency towards generating granulocytes and macrophages (Noetzli et al. 2019). MPP4, also termed lymphoid multipotent progenitors (LMPP), give rise to a common lymphoid progenitor (CLP). For MPP5, a close relationship with MPP1 has been reported, with MPP5 also being able to reconstitute MPP2-4 (Sommerkamp et al. 2021). CLP differentiate into T cells, B cells, natural killer cells (NK cells) and dendritic cells (DC). Eosinophils, basophils, neutrophils, macrophages and DC develop from GMP. MEP form red blood cells (RBC) or MK (Fig. 1). LT-HSC, IT-HSC, ST-HSC, MPP, CLP, CMP, GMP and MEP are collectively referred to as hematopoietic stem and progenitor cells (HSPCs).

### 1.1.1 Medullary erythropoiesis and megakaryopoiesis

Erythropoiesis is a dynamic and tightly regulated biological process in which RBC are generated from HSC. Initially, HSC are instructed to commit to the erythroid lineage, with the burst-forming unit-erythroid (BFU-E) as the first erythroid progenitor (Fig. 1). With the support of soluble factors, such as interleukin (IL) 3, stem cell factor (SCF) and granulocyte-macrophage colony-stimulating factor (GM-CSF), BFU-E can proliferate and further expand into colony-forming unit-erythroid (CFU-E) (Bot et al. 1998, Hattangadi et al. 2011). CFU-E survival and differentiation into erythroblasts are highly dependent on the kidney-derived hormone erythropoietin (EPO) (Wu et al. 1995, Hattangadi et al. 2011). The terminal erythroid maturation of erythroblasts to RBC occurs within specialized niches, termed erythroblastic islands (EBIs). These are comprised of a central macrophage surrounded by erythroblasts (Chasis and Mohandas 2008). The precise phenotypic characterization of the central macrophage is still under discussion. In mice, conditional ablation of $CD169^+$ macrophages significantly reduces the number of bone marrow erythroblasts and impairs recovery from anaemia, pointing to a crucial role of $CD169^+$ macrophages in erythropoiesis (Chow et al. 2013). Other studies additionally reported $F4/80^+$, vascular adhesion molecule 1 (VCAM-1) and EPO receptor (EPOR) as key markers of murine EBI macrophages (Jacobsen et al. 2014, Li et al. 2019).

In megakaryopoiesis, HSC progress through different progenitor stages, with MK giving rise to platelets (Fig. 1). However, there is increasing evidence that the HSC pool includes megakaryocyte-biased HSC, which have the ability to bypass progenitor stages and develop directly into megakaryocytes (Sanjuan-Pla et al. 2013, Yamamoto et al. 2013, Rodriguez-Fraticelli et al. 2018). Megakaryopoiesis is regulated by cytokines and a variety of bone marrow cells, such as stromal cells, sinusoidal bone marrow endothelial cells (BMEC), osteoblasts and macrophages (Avecilla et al. 2004, Alves-Rosa et al. 2003). Thrombopoietin (TPO), produced by the liver, osteoblast and stromal cells is the major regulator of MK progenitor (MkP) expansion and differentiation, while it is also essential for HSC maintenance (Hitchcock and Kaushansky 2014, Decker et al. 2018). While cytokines, such as IL-3, IL-6, IL-11 and leukemia inhibitory factor (LIF) have been shown to promote MK proliferation and maturation *in vitro*, they were not sufficient to rescue megakaryopoiesis in mice deficient in TPO ($Thpo^{-/-}$) or its receptor (c-Mpl) ($Mpl^{-/-}$) (Chen et al. 1998, Gainsford et al. 2000). In another study, CXC-motif-chemokine 12 (CXCL12) and fibroblast growth factor 4 (FGF-4) could restore megakaryopoiesis in $Thpo^{-/-}$ and $Mpl^{-/-}$ mice by supporting the interaction between

megakaryocytes and BMEC (Avecilla et al. 2004). *In vitro*, macrophages have been shown to promote homeostatic MK proliferation and platelet production, mainly by secreting GM-CSF that synergises with TPO (D'Atri et al. 2011). On the other hand, liposomal-encapsulated clodronate (LIP-CLOD) mediated depletion of macrophages has been reported to increase megakaryocyte numbers (Alves-Rosa et al. 2003).

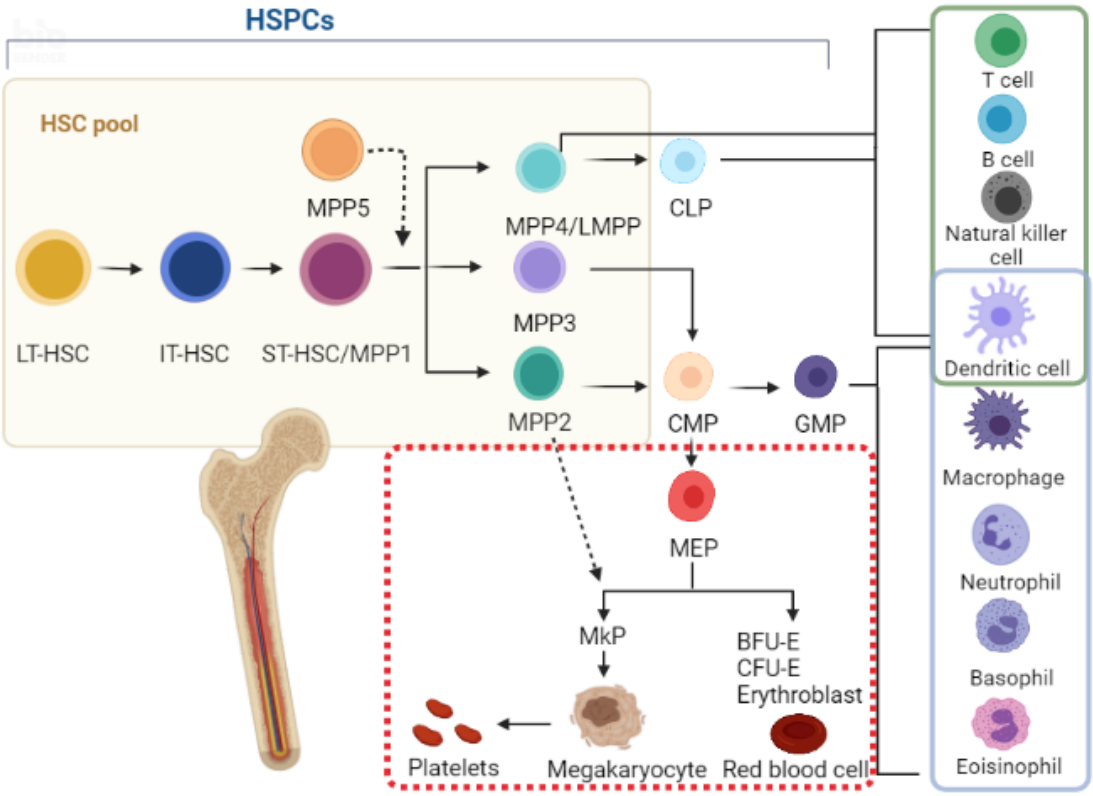


*Figure 1: Schematic representation of the hematopoietic hierarchy in steady state (adapted from Zhang et al. 2018). HSC – hematopoietic stem cell, HSPC – hematopoietic stem and progenitor cell, LT -long term, IT – intermediate-term, ST – short term, MPP – multipotent progenitor, LMPP – lymphoid multipotent progenitor, CLP – common lymphoid progenitor, CMP – common myeloid progenitor, GMP – granulocyte/macrophage progenitor, MEP – megakaryocyte/erythroid progenitor, MkP – megakaryocyte progenitor, BFU-E – burst forming unit erythroid, CFU-E – colony-forming unit erythroid. Created with BioRender.com.*

### 1.2 Infection-induced medullary haematopoiesis

In pathological conditions, such as infection and inflammation, haemorrhage and anaemia (Zhao and Baltimore 2015), bone marrow transplantation, cancer (Al Sayed et al. 2019), haematotoxic therapies (Sezaki et al. 2020) and genetic blood disorders (Bao et al. 2019), and during pregnancy (Inra et al. 2015), the ability of the haematopoietic system to adapt to stress events is crucial for survival.

When infectious agents (e.g. viruses, bacteria, fungi) enter the body, haematopoietic and non-haematopoietic cells can recognise pathogen-associated molecular patterns (PAMPs) with pattern recognition receptors (PRRs), such as Toll-like receptors (TLRs), RIG-I-like receptors and NOD-like receptors (NLRs). Upon activation of PRRs, cells respond by releasing pro-inflammatory cytokines and chemokines. These mainly include type I interferons (IFN-I), IL-6, IL-1β, tumour necrosis factor α (TNFα) and granulocyte-colony stimulating factor (G-CSF) (Boettcher and Manz 2017, Chavakis et. al 2019).

While local infections can be effectively cleared by innate immune cells, the problem arises once the pathogen can not be contained and spreads systemically. Systemic infection is characterized by elevated neutrophils, myeloid cells and myeloid precursors in the peripheral blood (Boettcher and Manz 2017). The vast consumption of these cell populations in the periphery enhances the demand for their replenishment. In the bone marrow, HSPC respond by increasing their proliferative rate, mobilizing to the periphery and differentiating preferentially towards cells of the myeloid lineage. This shift favouring myeloid cell production, while decreasing lymphopoiesis, is termed emergency myelopoiesis (Mitroulis et al. 2018). It is known that HSPC can respond to infection regardless of peripheral cytopenia (King and Goodell 2011). As they also possess functional TLRs (Nagai et al. 2006, Megías et al. 2012) and express various cytokine receptors, HSPCs can be activated directly by PAMP or by cytokines (King and Goodell 2011, Chavakis et al. 2019).

Following TLR-mediated stimulation, HSPCs are also able to produce cytokines, mainly IL-6 (Zhao and Baltimore 2015). IL-6 is an important regulator of infection-induced haematopoiesis and is known to induce myeloid cell differentiation as well as HSC proliferation (Zhao et al. 2014). Entry of HSC into the cell cycle is also promoted by IFNα and IFNγ (Essers et al. 2009, Baldridge et al. 2010). Other prominent factors that contribute to emergency myelopoiesis during infection include TNFα, IL-1β, IL-27, IFNγ, G-CSF, macrophage-colony stimulating factor (M-CSF) and GM-SCF (Zhao et al. 2014, Chavakis et al. 2019, Hormaechea-Agulla et al. 2020). G-CSF mainly acts on CMP and GMP, instructing them to differentiate into

granulocytes, while M-CSF stimulates GMP to differentiate into macrophages (Kovtonyuk et al. 2016). IFNγ has been shown to act on CMP and GMP, promoting their differentiation into monocytes, but not granulocytes (De Bruin et al. 2012).

### 1.3 Infection-induced extramedullary haematopoiesis in the spleen

In consequence of haematopoietic stress caused by systemic infection, HSPC are mobilized from the bone marrow to alternative sites of haematopoiesis. The process in which mature blood cells are formed outside the bone marrow is referred to as extramedullary haematopoiesis (EMH) (Kim 2010).

The spleen, a secondary immune organ consisting of the white pulp, marginal zone and red pulp (Mebius and Kraal 2005), is a common site of infection-induced EMH (Chiu et al. 2015). Various bacterial and parasitic infections have been shown to induce splenic EMH, which is characterized by the enlargement of the spleen, known as splenomegaly. Another hallmark of splenic EMH is the increase of cells of the myeloid, megakaryocyte and erythroid lineage (Chiu et al. 2015). For example, mice infected with the obligate intracellular bacterium *Anaplasma phagocytophilum* exhibit an impaired bone marrow haematopoiesis, whereas increased numbers of megakaryocytes and erythroid progenitors are observed in the spleen (Johns et al. 2009). *Ehrlichia muris* and *Salmonella spp.* infection are characterized by elevated splenic erythroid progenitors (MacNamara et al. 2009, Jackson et al. 2010). Splenic myelopoiesis is also promoted during the acute infection with *Plasmodium chabaudi*, a malaria-causing parasite in rodents, with an increase of CMP and GMP (Belyaev et al. 2013). A more recent study, using a mouse model of *Trypanosoma cruzi* oral infection, reported splenomegaly with an increase in immature granulocytes and megakaryocytes (Marins-Dos-Santos et al. 2022). While a lot is known about infection-induced splenic EMH during bacterial and parasitic infections, only a few studies addressed it in the context of viral infections. Splenomegaly is commonly developed during acute human cytomegalovirus (HCMV) infection, which in some cases can result in spleen rupture (Alliot et al. 2001, Duarte et al. 2003). In mice infected with murine cytomegalovirus (MCMV), splenomegaly was associated with the induction of EMH, characterized by a pronounced increase of cells of the myeloid and erythroid lineage (Jordan et al. 2013).

During EMH, HSPCs are found localized in the proximity of spleen sinusoids in the red pulp, where spleen sinusoidal endothelial cells (EC) and transcription factor 21 (Tcf21) expressing perisinusoidal stromal cells form a perivascular niche (Fig. 2) (Kiel et al. 2005, Inra et al. 2015).

Upon induction of EMH, both cell types start to proliferate and secrete key haematopoietic factors, such as SCF and FGF-4, which are essential in haematopoietic niche maintenance and HSPC retention (Inra et al. 2015, Wilson and Trumpp 2006, Johns and Christopher 2012). *Tcf21*$^{+}$ stromal cells additionally produce CXCL12, which is mainly involved in HSPC attraction (Fig. 2) (Inra et al. 2015). More recently, splenic mesenchymal cells expressing the T cell leukemia homeobox 1 (Tlx1) protein, a vital transcription factor in spleen organogenesis, have also been implicated in EMH, as mice with a conditional deletion of *Tlx1* failed to induce EMH in response to LPS treatment (Oda et al. 2018).

Macrophages are important components of the splenic haematopoietic niche. Through adhesion molecules, such as VCAM1, RPM interact with HSC and erythroblasts (Dutta et al. 2015). Red pulp macrophages (RPM) are the main source of bone morphogenic protein 4 (BMP4), a protein required during stress erythropoiesis to promote expansion of erythroid progenitors (Fig. 2) (Millot et al. 2010, Perry et al. 2007). In mouse models of polycythemia vera, LIP-CLOD mediated depletion of macrophages impairs stress erythropoiesis (Ramos et al. 2013). Similarly, conditional ablation of CD169$^{+}$ macrophages results in reduced erythroid recovery in the spleen after bone marrow transplantation (Chow et al. 2013). Macrophages are also constitutents of EBIs and facilitate terminal erythroblast maturation (Fig. 2) (Chasis and Mohandas 2008).

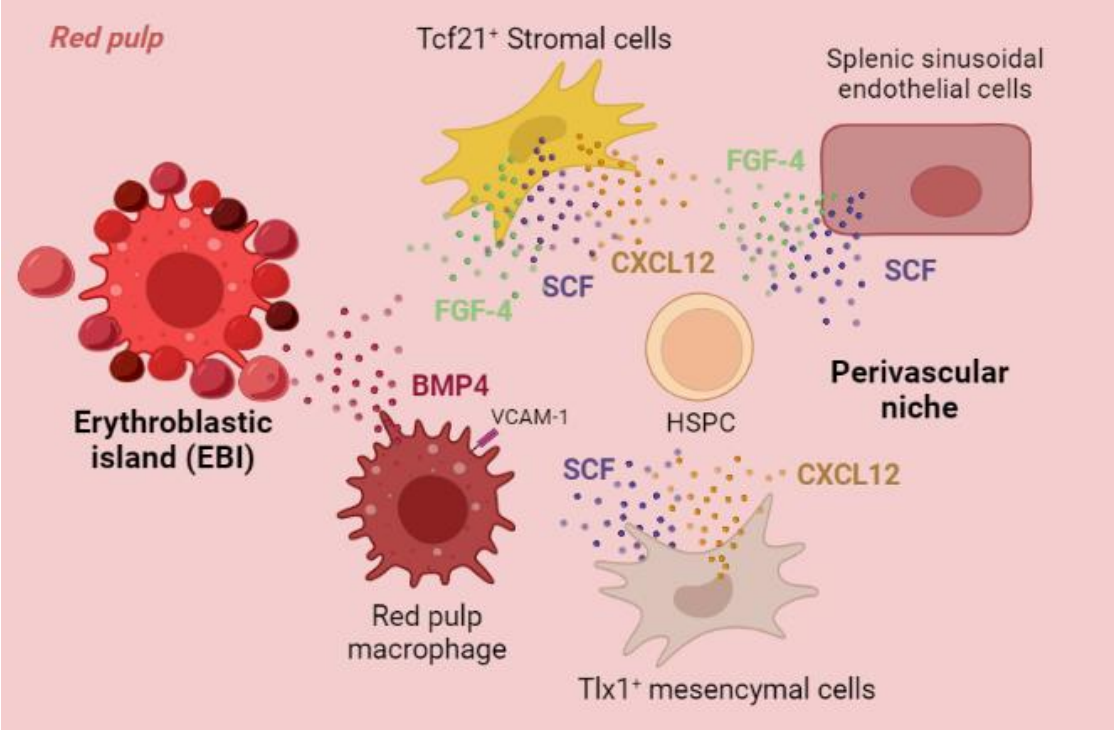


*Figure 2: Schematic representation of the splenic haematopoietic niche; the perivascular niche and erythroblastic islands. HSPC = haematopoietic stem and progenitor cell, Tcf21 = transcription factor 21, Tlx1 = T cell Leukemia Homeobox 1, CXCL12 = CXC-motif-chemokine 12, SCF = stem cell factor, FGF-4 = fibroblast growth factor 4, BMP4 = bone morphogenic protein 4, VCAM1 = vascular adhesion molecule 1. Created with BioRender.com.*

### 1.4 The JAK-STAT signaling pathway

In mammals, there are four members of the Janus kinase (JAK) family (JAK1, 2, 3 and tyrosine kinase 2 (TYK2)) and seven members of the signal transducers and activators of transcription (STATs) family (STAT1, 2, 3, 4, 5A, 5B and 6) (Aaronson and Horvath 2002). Together, JAKs and STATs form a signal transduction pathway that is known as the JAK-STAT pathway.

The JAK-STAT pathway connects extracellular signals from the cell surface to transcriptional changes of target genes in the nucleus and is involved in the regulation of fundamental cellular processes, such as cell growth, proliferation, differentiation and apoptosis. It can be activated by a variety of hormones, growth factors and cytokines (Stark et al. 2018). After a ligand binds to its corresponding receptor, JAKs bound to the receptor's intracellular domains autophosphorylate and phosphorylate tyrosine (Tyr) residues on receptor chains, creating docking sites for the Src-homology 2 (SH2) domain of the STATs. Upon binding, STATs get phosphorylated and translocate to the nucleus as homodimers or heterodimers. In the nucleus,

the STAT dimers bind to the target promotors to activate gene expression (Aaronson and Horvath 2002).

### 1.4.1 Signal transducer and activator of transcription 1

STAT1 is the key effector of all types of IFNs, activating the transcription of several hundred IFN-stimulated genes (ISG) (Fig. 3) (Ramana et al. 2000, Najjar and Fagard 2010). In viral infections, cells react by producing IFNs to prevent viral replication and spread to yet-uninfected cells (Samuel 2001). There are three types of IFNs in humans and mice, type I IFNs (FNα subtypes, IFNβ, IFNε, IFNκ, IFNω), type II IFNs (FNγ as the only member) and type III IFNs (IFN-λ1, IFN-λ2, IFN-λ3 and, in humans, IFN-λ4) (Pestka et al. 2004, Platanias 2005, Wack et al. 2015). STAT1 is also involved in the signal transduction of IL-21, IL-27 and IL-35 (Boisson-Dupuis et al. 2012, Vignali and Kuchroo 2012).

In IFN signaling, STAT1 activation and interaction with its gene targets depends on the type of IFN (Fig. 3). Type I IFNs bind to type I IFN receptor (IFNAR), consisting of two subunits, IFNAR1 and IFNAR2. It mainly induces the activation of STAT1 and STAT2, which form a transcriptional complex with the interferon regulatory factor 9 (IRF9), called interferon-stimulated gene factor 3 (ISGF3), which binds to IFN-stimulated response element (ISRE) to induce the transcription of ISG (Fig. 3) (Najjar and Fagard 2010). Type III IFNs bind to the IL-10Rβ and IFNLR1 receptor chains, activating the same transcriptional complexes as type I IFN (Fig. 3) (Lazear et al. 2019). Type II IFNs bind to the IFNγ receptor (IFNGR) with IFNGR1 and IFNGR2 as its functional units (Kotenko et al. 1995) and mainly activate STAT1 homodimers, also called gamma-IFN activated factor (GAF) (Najjar and Fagard 2010). GAF translocates to the nucleus where it binds to gamma activated sequence (GAS) motifs and induces ISG transcription (Fig. 3) (Au-Yeung et al. 2013, Darnell et al. 1994).

STAT1 has multiple biological functions. It regulates cell growth (Bromberg et al. 1996, Dimberg et al. 2003), cell differentiation (Kim et al. 2003), apoptosis (Kumar et al. 1997, Stephanou and Latchman 2005) and tumourigenesis (Kovacic et al. 2006, Meissl et al. 2017). STAT1 is best known for its role in the immune response. Numerous studies have shown that mice deficient of STAT1 are highly susceptible to many bacterial, parasitic and viral infections (Meraz et al. 1996, Decker et al. 2002), among them *Mycobacterium tuberculosis* (Sugawara et al. 2004), *Toxoplasma gondii* (Gavrilescu et al. 2004) and MCMV (Gil et al. 2001). Similarly, STAT1 deficient patients are severely immunocompromised and have a low life expectancy (Boisson-Dupuis et al. 2012). Recently, its regulatory role in maintaining key molecular

programs of homeostatic HSCs has been described (Li et al. 2021)

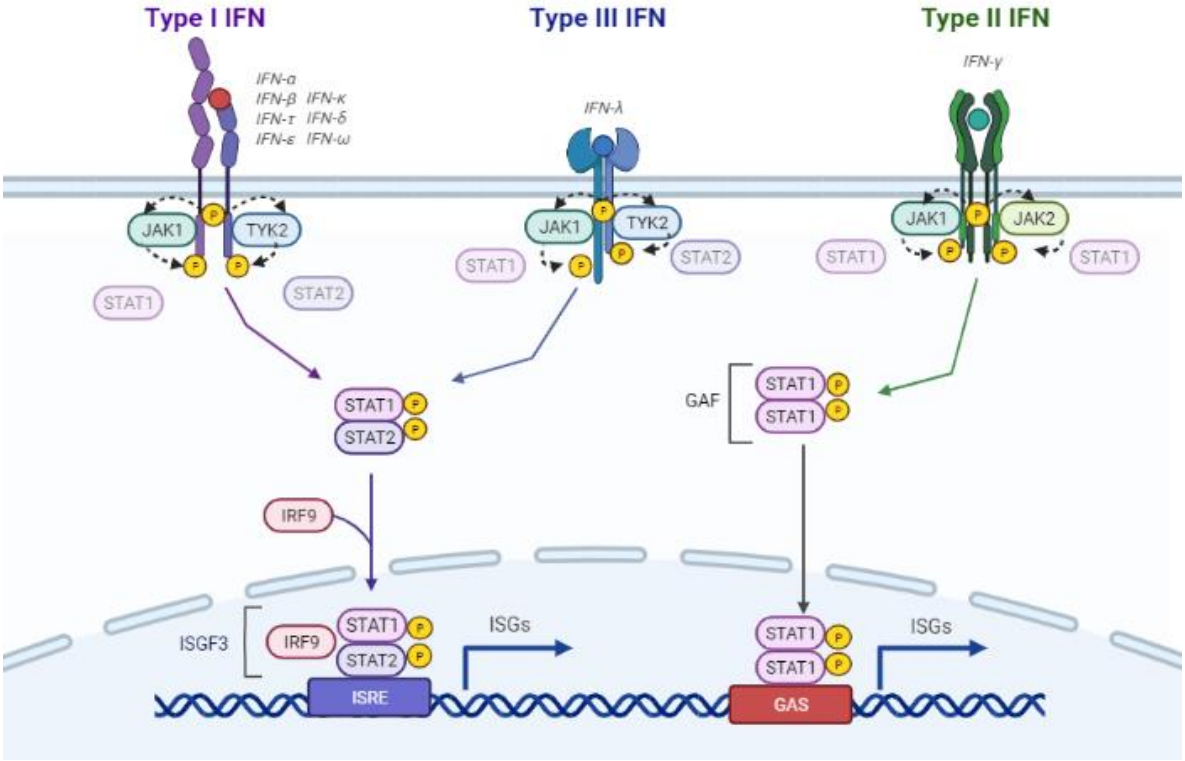


*Figure 3: The signal transducer and activator of transcription 1 (STAT1) is an essential component of the interferon (IFN) signalling pathway (adapted from Najjar and Fagard 2010). JAK 1/2 – Janus kinase, TYK2 – tyrosine kinase 2, P – phosphate, IRF9 – interferon regulatory factor 9, ISGF3 – interferon stimulated gene factor 3, ISRE – interferon stimulated response element, ISGs – IFN stimulated genes, GAF – gamma IFN activated factor, GAS – gamma activated sequence. Created with BioRender.com.*

## 2. Aim of the study

Previous studies in our laboratory have shown that mice with conditional ablation of *Stat1* in the myeloid lineage (monocytes, macrophages and polymorphonuclear neutrophils) (*Stat1*$^{\Delta M/PMN}$) exhibit impaired EMH in the spleen during MCMV infection (Gawish et al. 2019). In particular, numbers of erythroblasts and megakaryocytes in the spleen of *Stat1*$^{\Delta M/PMN}$ were significantly lower when compared to their littermate controls (*Stat1*$^{fl/fl}$), suggesting that myeloid STAT1 promotes splenic erythropoiesis and megakaryopoiesis.

To better understand the mechanisms, we focused on the immediate precursors of erythroblast and megakaryocytes, CFU-E and MkP, respectively. The aim of the thesis was to explore the abundance and proliferative state of CFU-E and MkP in the spleen of MCMV infected *Stat1*$^{\Delta M/PM}$ and *Stat1*$^{fl/fl}$ mice. In parallel, we wanted to assess the abundance and proliferation of CFU-E and MkP in the bone marrow, to investigate whether differences in splenic progenitors between *Stat1*$^{\Delta M/PMN}$ and controls correlate with differences in the bone marrow. In addition, levels of cytokines and chemokines involved in erythropoiesis and megakaryopoiesis should be measured in spleen homogenates at day 3 and 5 after MCMV infection and PBS controls.

# 3. Material and methods

## 3.1 Material

*Table 1. Equipment*

| Name | Source | Identifier |
|---|---|---|
| Tubes 50mL | Greiner Bio-One | Cat. #210261 |
| Tubes 15mL | Sarstedt | Cat. #62.554.502 |
| SafeSeal micro tube 2 mL | Sarstedt | Cat. #72.695.500 |
| Tubes 1,5 mL | Sarstedt | Cat. #72.690.001 |
| Tubes 0,5 mL | Sarstedt | Cat. #72.699 |
| FACS tubes | Falcon | Cat. #352008 |
| MACS Smart strainers 100 µm | Miltenyi | Cat. #130-110-917 |
| Pre-Separation filter 70 µm | Miltenyi | Cat. #130-095-823 |
| LS columns | Miltenyi | Cat. #130-042-401 |
| Omnifix®-F 1mL syringe | B. Braun | Cat. #9161406V |
| Sterican® Heparin/Tuberkulin G25 x 5/8", Ø 0,50 x 16 mm needle | B. Braun | Cat. #4657853 |
| 96-Well Plates | Falcon | Cat. #353075 |
| TC20 Automated Cell Counter | Bio-Rad | Cat. #1450102 |
| 96-well Hand-Held Magnetic Plate Washer | Thermo Fisher | Cat. #EPX-55555-000 |
| MACS®MultiStand | Miltenyi | Cat. #130-042-303 |
| 1600 MiniG® | SPEX®sampleprep | NA |
| Luminex | Bio-Rad | NA |
| CytoFLEX | Backman Coulter | NA |

*Table 2. Media and buffers*

| Name | Company | Identifier |
|---|---|---|
| RPMI-1640 Medium | Sigma-Aldrich | Cat. #R5757 |
| Dulbecco's Phosphate Buffered Saline (PBS) | Sigma-Aldrich | Cat. #D8537 |
| autoMACS Running Buffer | Miltenyi | Cat. #130-091-221 |
| ProcartaPlex Cell Lysis Buffer | Thermo Fisher | Cat. #EPX-99999-000 |
| Intracellular Staining Permeabilization Wash Buffer (10X) | BioLegend | Cat. #421002 |
| Fixation buffer | BioLegend | Cat. #420801 |
| Red Blood Cell Lysing Buffer | Sigma-Aldrich | Cat. #R7757 |

*Table 3. Chemicals, reagents and commercial assays*

| Name | Manufacturer | Identifier |
|---|---|---|
| Collagenase D | Sigma Aldrich | Cat. #11088866001 |
| DNase I | Sigma Aldrich | Cat. #11284932001 |
| ProcartaPlex Mouse Basic Kit 96 tests | Thermo Fisher | Cat. #20440-901 |
| Fetal bovine serum (FBS) (heat-inactivated) | Gibco | Cat. #10270-098 |
| Trypan Blue solution | Sigma-Aldrich | Cat. #T8154 |
| Pierce BCA Protein assay kit | Thermo Fisher | Cat. #23225 |
| Pierce™ Protease and Phosphatase Inhibitor mini tablets | Thermo Scientific | Cat. #A32959 |

| | | |
|---|---|---|
| PMSF | Thermo Scientific | Cat. #36978 |
| Direct Lineage Depletion Kit | Miltenyi Biotec | Cat. #130-110-470 |
| DAPI (4',6-Diamidino-2-Phenylindole, Dihydrochloride) | Sigma-Aldrich | Cat. #D9542 |
| Fixable viability dye | Thermo Fisher Scientific | Cat. #65-0865-18 |
| IL-6 Mouse ProcartaPlex™ Simplex Kit | Thermo Fisher | Cat. #EPX01A-20603-901 |
| IL-3 Mouse ProcartaPlex™ Simplex Kit | Thermo Fisher | Cat. #EPX01A-26035-901 |
| IFN alpha Mouse ProcartaPlex™ Simplex Kit | Thermo Fisher | Cat. #EPX01A-26027-901 |
| IFN beta Mouse ProcartaPlex™ Simplex Kit | Thermo Fisher | Cat. #EPX01B-26044-901 |
| IFN gamma Mouse ProcartaPlex™ Simplex Kit | Thermo Fisher | Cat. #EPX01A-20606-901 |
| GM-CSF Mouse ProcartaPlex™ Simplex Kit | Thermo Fisher | Cat. #EPX01A-20612-901 |
| LIF Mouse ProcartaPlex™ Simplex Kit | Thermo Fisher | Cat. #EPX01A-26040-901 |
| Mouse IL-11 ELISA Kit | Abcam | Cat. #ab215084 |
| Mouse Thrombopoietin ELISA Kit (TPO) | Abcam | Cat. #ab100748 |
| Mouse Erythropoitin ELISA Kit (EPO) | Abcam | Cat. #ab119593 |
| Mouse SDF1 ELISA Kit | Abcam | Cat. #ab100741 |
| Mouse SCF ELISA Kit | Abcam | Cat. #ab197750 |

*Table 4. Flow cytometry antibodies*

| Name | Fluorochrome | Clone | Source | Identifier |
|---|---|---|---|---|
| Rat monoclonal antibody CD105 (Endoglin) | APC | MJ7/18 | Thermo Scientific | Cat. #17-1051-82 |
| Rat monoclonal antibody CD150 | PE | mShad150 | Thermo Scientific | Cat. #12-1502-82 |
| Rat monoclonal antibody CD16/32 | unconjugated | 93 | Thermo Scientific | Cat. #14-0161-82 |
| Rat monoclonal antibody CD16/32 | PerCP-Cyanine5.5 | 93 | Thermo Scientific | Cat. #45-0161-82 |
| Armenian Hamster monoclonal antibody CD3ε | PE-Cyanine7 | 145-2C11 | Thermo Scientific | Cat. #25-0031-82 |
| Rat monoclonal antibody Ter119 | PE-Cyanine7 | TER-119 | Thermo Scientific | Cat. #25-5921-82 |
| Rat monoclonal antibody CD19 | PE-Cyanine7 | 6D5 | BioLegend | Cat. #115533 |
| Armenian hamster antibody CD11b | PE-Cyanine7 | N418 | Thermo Scientific | Cat. #25-0114-82 |
| Rat monoclonal antibody CD117 (c-Kit) | Super Bright 780 | 2B8 | Thermo Scientific | Cat. #78-1171-82 |
| Ki-67 FITC set B56 | FITC | NA | BD BioSciences | Cat. #556026 |

| *Table 5. Experimental mice models* | | |
|---|---|---|
| **Name** | **Source** | **Identifier** |
| *Stat1* $^{fl/fl}$ | (Wallner et al. 2012) | N/A |
| *Stat1*$^{\Delta M/PMN}$ | (Wallner et al. 2012) | N/A |

| *Table 6. Virus strain* | | |
|---|---|---|
| **Name** | **Source** | **Identifier** |
| Salivary gland murine cytomegalovirus (SG - MCMV) | American Type Culture collection | ATCC®VR194 |

| *Table 7. Software* | | |
|---|---|---|
| **Name** | **Source** | **Identifier** |
| CytExpert | Beckman Coulter Life Sciences | N/A |
| Prism 9.4.1 | GraphPad Software | N/A |

## 3.2 Methods

### 3.2.1 Mice and virus injection

Mice lacking STAT1 specifically in cells of the myeloid lineage (monocytes, macrophages and polymorphonuclear neutrophils) *Stat1*$^{\Delta M/PMN}$ (*Stat1*$^{flox/flox}$/*LysMCre*) were described previously (Wallner et al. 2012). *Stat1*$^{fl/fl}$ mice (*Stat1*$^{flox/flox}$) were used as littermate controls. Mice were on a C57BL/6N background. All mice were sex-matched, aged between 9 and 12 weeks and bred under specific pathogen-free conditions at the University of Veterinary Medicine Vienna according to the Federation of European Laboratory Animal Science Associations (FELASA) guidelines. Mice were injected intraperitoneally (i.p) with 200 µL of salivary gland-derived murine cytomegalovirus (SG-MCMV) at a dose of 5 x $10^4$ PFU/mouse. As a control, PBS was

injected. All in vivo experiments were performed by trained personnel. The animal experiments were approved by the institutional ethics and animal welfare committee and the national authority, according to §§ 26ff. of Animal Experiments Act, Tierversuchsgesetz 2012-TVG 2012 (BMWFW 68.205/0032-WF/II/3b/2014).

### 3.2.2 Experimental set up

Spleen and femurs were harvested on days 3 and 5 post infection (p.i) (Fig. 5). The spleen was weighed and stored in PBS for splenocyte isolation. A small piece of the spleen was cut off, weighted, shock-frozen in liquid nitrogen and stored at - 80 °C until homogenization. Both legs were stored in PBS for the isolation of bone marrow cells. The cells from the bone marrow cell suspension were counted after red blood cell lysis.

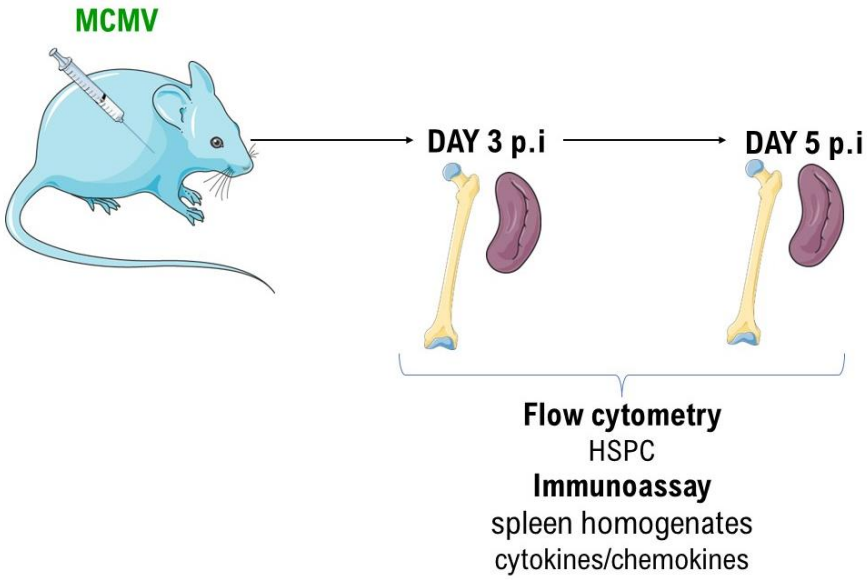


*Figure 4: Schematic representation of the experimental set up.*

### 3.2.3 Cell preparation for flow cytometry

#### 3.2.3.1 Isolation of splenocytes

The spleen was injected with 1-1.5 mL of pre-warmed digestion medium (RPMI1640 medium, 100 µg/mL and 100 U/mL penicillin-streptomycin, 2% FBS, 0.1 mg/mL Collagenase D, 0.02 mg/mL DNAse I) minced into pieces with scissors and incubated at 37 °C with 5% $CO_2$ for 30 min. The digested spleens were filtered through a 100 µm cell strainer placed over a 50 mL tube kept on ice. Tissue pieces that remained on the strainer were mashed using a syringe

plunger and subsequently washed with ice-cold MACS/2.5 % FBS buffer and centrifuged at 400 x *g* for 5 min. The pellet was resuspended in 2 mL of Red Blood Cell Lysing Buffer and incubated for 5 min at RT. The reaction was stopped by the addition of 20 mL MACS/2.5 % FBS buffer. The cell suspension was filtered through a 100 µm cell strainer into a new 50 mL tube and centrifuged at 400 x *g* for 5 min. The pellet was resuspended in 20 mL of MACS/2.5 % FBS buffer and the cells were counted. 4 x $10^7$ of the cells were taken for lineage depletion, and the cells were resuspended in 160 µL of MACS/2.5 % FBS buffer. Next, 40 µL of the Direct Lineage Cell depletion Kit cocktail was added and samples were incubated at 4 °C for 10 min. After the incubation step, 2 mL of MACS/2.5 % FBS Buffer were added to each sample. The kit contains MicroBeads that are conjugated to monoclonal antibodies against CD5, CD11b, CD45R (B220), Gr-1 (Ly-6G/C), 7-4, and Ter-119. Cells positive for these markers were removed by magnetic separation and discarded. The remaining lineage negative cells were counted and subjected to cell surface staining with antibodies against different markers to analyse CFU-E and MkP. Viable CFU-E were defined as: $CD3\varepsilon^-$, $CD19^-$, $CD11b^-$, $Ter119^-$, $CD16/32^-$, $cKIT^+$, $CD105^+$ and $CD150^-$. Viable MkP were defined as $CD3\varepsilon^-$, $CD19^-$, $CD11b^-$, $Ter119^-$, $CD16/32^-$, $cKIT^+$ $CD45^+$, $CD150^+$, $CD41^+$. All antibodies were diluted 1:200 and the viability-dye was diluted 1:1000. The cells were incubated for 25 min at 4 °C, after which cells were washed with MACS/2.5 % FBS and centrifuged at 400 x *g* for 5min. Cells were fixed with 250 µL Fixation Buffer and incubated at RT for 15 min in the dark. After the fixation step, samples were washed and centrifuged at 400 x *g* for 5min. The samples were kept at 4 °C over night. Next day, cells were permeabilized with 1x Permeabilization Buffer and centrifuged. To access the proliferative status of the cells, intracellular staining with DAPI (2 µg/mL) and anti-Ki-67 (1:25 dilution) was performed, followed by an incubation period of 30 min in the dark at RT. After the incubation, cells were washed, centrifuged, resuspended in 200 µL PBS and analysed with a flow cytometry analyser.

#### 3.2.3.2 Isolation of bone marrow cells

After cleaning the femurs were grind with a pestle and mortar in ice-cold PBS. The crushed bones were filtered through a 100 µm cell strainer. Using a syringe plunger the bone fragments that remained on top of the strainer were mashed and subsequently washed with PBS. The samples were centrifuged at 400 x *g* for 5 min. The pellet was resuspended in 1 mL of Red Blood Cell Lysis Buffer. The suspension was left at RT for 5 min, after which the reaction was stopped by the addition of 10 mL of PBS. The suspension was filtered through a 100 µm cell

strainer, followed by another centrifugation step at 400 x *g* for 5 min. The resulting pellet was resuspended in 20 mL of MACS/2.5 % FBS buffer. After counting, 5 x $10^6$ cells were stained with the surface staining antibody mix to identify the CFU-E and MkP (see section 3.2.3.1). Cells were fixed with 250 µL Fixation Buffer, incubated at RT for 15 min in the dark, washed and centrifuged at 400 x *g* for 5min. The samples were kept at 4 °C over night. Next day, cells were permeabilized with 1x Permeabilization Buffer, centrifuged and intracellular staining was performed (see section 3.2.3.1). After the incubation the cells were washed, centrifuged, resuspended in 200 µL PBS and analysed with a flow cytometry analyser.

### 3.2.3.3 Gating strategy

For the bone marrow samples at least 1.5 x $10^6$ cells were recorded. For the depleted spleen samples as much cells as possible were recorded. The representative FACS plots with the gating strategy to identify the CFU-E and MkP populations are depicted in Figure 6 and 7. From all the cells duplets, dead cells and lineage positive cells ($CD3e^+$, $Ter119^+$, $CD19^+$, $CD11b^+$) were gated out. The CFU-E population was defined as $Lin^-$, $CD16/32^-$, $cKIT^+$, $CD105^+$, $CD150^-$ (Fig. 5), while the MkP population was defined as $Lin^-$, $CD45^+$, $CD150^+$ and $CD41^+$ (Fig. 6).

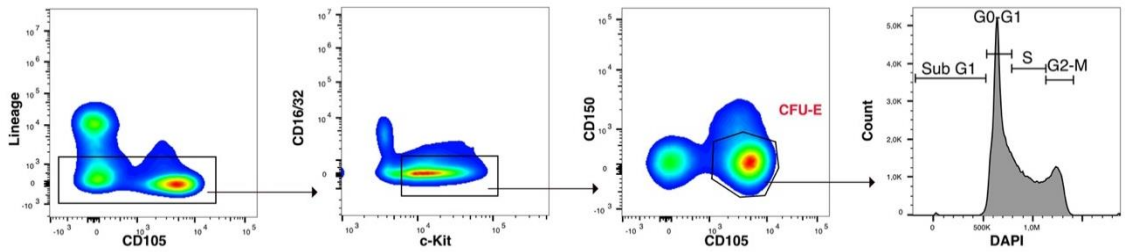


*Figure 5: Gating strategy for colony forming unit erythroid (CFU) with DAPI intensity histogram for the determination of cell cycle phases.*

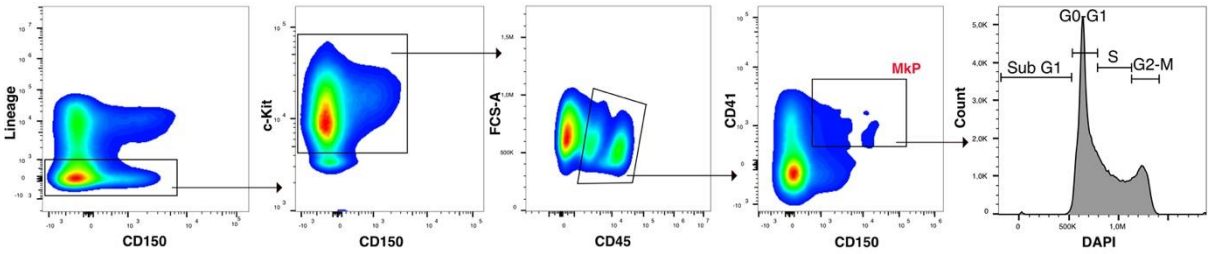


*Figure 6: Gating strategy for megakaryocyte progenitors (MkP) with DAPI intensity histogram for the determination of cell cycle phases.*

### 3.2.4 Homogenization of spleen

Spleen tissue pieces were stored at -80 °C until homogenization. The Cell Lysis Buffer was prepared by adding one tablet of protease and phosphatase inhibitors per 10 mL of buffer. Before use, PMSF at a working concentration of 1mM was added to the Cell Lysis Buffer. The amount of Cell Lysis Buffer added to each sample was calculated based on the tissue weight (5µL per 1 mg of tissue). Thereafter 2 magnetic beads were added per sample and samples were homogenized in the 1600 MiniG® tissue homogenizer at 1500 rpm for 30 seconds. The beads were removed by a magnet and the lysates were pulse-sonicated at 72 kHz for 10 seconds. The sonicated samples were incubated on ice for 5 to 10 min. Lysates were spun down at 16110 × *g* at 4°C for 10 min to pellet debris. The protein concentration in the supernatant was determined with a bicinchoninic acid (BCA) assay.

### 3.2.5 Bicinchoninic acid (BCA) assay

To determine the protein concentration, a BCA assay was performed according to the manufacturer's instructions. A set of standards was prepared by diluting bovine serum albumin (BSA) in PBS to achieve a working range of 20 – 2000 µg/mL. The samples were diluted 1:10 in PBS. Working reagent (WR) was prepared by mixing the provided BCA Reagent A with BCA reagent B (50:1, Reagent A:B). 25 µL of each standard or sample was pipetted in triplicates into a 96 well microplate. 200 µL of WR was added per well and the plate was placed on a plate shaker for 30 seconds. The plate was covered and incubated at 37 °C for 30 min. The absorbance was measured at 562 nm immediately after the incubation. Based on the measured absorbance, the protein content of samples was calculated and samples were diluted to a final concentration of 10 mg/mL protein per sample. Another BCA assay was performed to validate the concentration.

### 3.2.6 ELISA

Assays were performed according to the manufacturer's instructions. Briefly, the standards were prepared by reconstituting the stock standard of the given analyte with the same diluent used for diluting the samples. The working range of the standards was specific for each analyte. Based on the results of pre-runs of each analyte the samples were diluted 1:2 or 1:3 with the specified diluent. Depending on the analyte, 50 µL or 100 µL of the standards and diluted samples were added to the wells. After a series of incubation, washing and adding capture/detector antibodies the absorbance was measured at 450 nm.

### 3.2.7 Luminex

The Luminex immunoassay was performed using the commercially available kit according to the manufacturer's instructions. For the measuring of cytokines with Luminex all samples had the same protein concentration (10 mg/mL). Standards were prepared by pooling the Standard Mix A (IL-6, IFNγ, GM-CSF), Standard Mix 1B (IL-3, Lif, IFNα) and IFNβ Standard and performing a 2.5-fold serial dilution. The standards were diluted with the Universal Assay Buffer provided in the kit and stored on ice. The Wash Buffer was equilibrated to RT and diluted 1:10 with $ddH_2O$. The Magnetic bead mix was prepared by adding 1 µL/per sample of 50x analyte specific magnetic beads into 1x Wash Buffer. The plate was placed on a handheld magnetic washer and 50 µL of the magnetic bead mix was pipetted into each well. After 2 min the plate was inverted followed by a wash step with 150 µL of 1x Wash buffer. 25 µL of standards and samples were pipetted into dedicated wells. The plate was sealed and incubated for 30 min at 500 rpm at RT after which it was incubated at 4 °C over night. On the next day the plate was first left to shake at 500 rpm at RT for 30 min and then washed 3 times with 150 µL of the 1x Wash Buffer. The 1x Detection Antibody Mixture was prepared by adding 0.5 µL of each analyte specific detection antibody per sample, diluted with 1x Detection Antibody Diluent. 25 µL of the 1x Detection Antibody Mixture were added into each well. The plate was sealed and incubated for 30 min at 500 rpm at RT, followed by 3 washing steps with 150 µL of 1x Wash buffer. To each well 50 µL of Streptavidin-PE was added. The plate was sealed and incubated for 30 min at 500 rpm at RT, followed by 3 washing steps with 150 µL of 1x Wash buffer. Finally, 120 µL of the provided Reading Buffer was added to each well and the plate was shaken at 500 rpm for 5 min at RT.

### 3.2.8 Statistical analysis

Statistical analyses were performed with GraphPad Prism 9.4.1, using a t-test on square root transformed data (cell abundance differences between the genotypes), one-way analysis of variance (ANOVA) on square-root transformed data (differences in proliferative state between the genotypes) and t-test on untransformed data (differences in cytokine levels between the genotypes). Differences with a p-value ≤ 0.05 were interpreted as significant (* $p < 0.05$; ** $p < 0.01$; *** $p < 0.001$). p-values between 0.05 and 0.1 are indicated in the graphs.

# 4. Results

## 4.1 STAT1 signaling in myeloid cells does not affect the abundance and proliferation of CFU-E in the spleen and the bone marrow during MCMV infection

Previous studies in our laboratory have shown that upon infection with MCMV, *Stat1*$^{\Delta M/PMN}$ mice have decreased erythroblasts in the spleen compared to littermate controls, while the abundance of erythroblasts in the bone marrow was not affected (Gawish et al. 2019). To better understand the mechanism, we analysed the abundance and proliferative state of the immediate precursors of erythroblasts, the CFU-E, in the spleen and bone marrow of *Stat1*$^{\Delta M/PMN}$ and *Stat1*$^{fl/fl}$ mice using flow cytometry. CFU-E were detected in the spleens of MCMV infected *Stat1*$^{\Delta M/PMN}$ and *Stat1*$^{fl/fl}$ mice but not in PBS treated mice, confirming the induction of extramedullary erythropoiesis in response to MCMV infection (Fig. 7A). The frequency of splenic CFU-E at both time points p.i. did not significantly differ between mice of the two genotypes (Fig. 7A).

The proliferation of CFU-E was analysed by measuring cell cycle distribution using DAPI staining. Most of the CFU-E were in the G0-G1 and S phase at 3 days and 5 days p.i., with no differences between *Stat1*$^{\Delta M/PMN}$ and *Stat1*$^{fl/fl}$ mice (Fig. 7B). At day 3 p.i., around 5-10% of CFU-E were in the sub-G phase, which indicates cell death or cell cycle arrest (Fig. 7B). This cell population was slightly increased in *Stat1*$^{\Delta M/PMN}$ compared to *Stat1*$^{fl/fl}$ mice, albeit it did not reach our threshold of statistical significance (Fig. 7B).

In the bone marrow, the frequency of CFU-E did not change in response to MCMV infection and there were no differences between *Stat1*$^{\Delta M/PMN}$ and *Stat1*$^{fl/fl}$ mice (Fig. 7C). Similar to the spleen, most bone marrow CFU-E were in the G0-G1 and S phase of the cell cycle, with no differences between *Stat1*$^{\Delta M/PMN}$ and *Stat1*$^{fl/fl}$ mice (Fig. 7D). Taken together, these data indicate that the abundance and proliferative state of CFU-E in the spleen and bone marrow during MCMV infection are not affected by STAT1 signalling in myeloid cells.

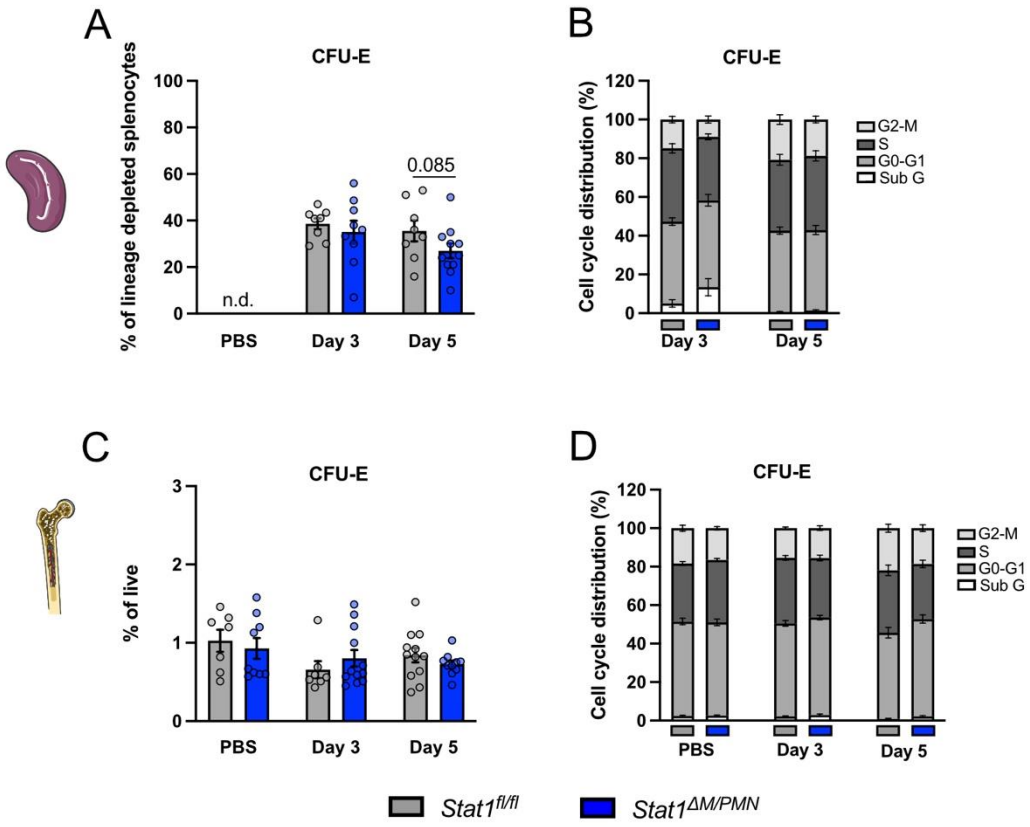


*Figure 7: STAT1 in myeloid cells does not affect spleen and bone marrow CFU-E abundance and proliferation upon MCMV infection. Mice were infected with 5 x $10^4$ PFU/mL of SG-MCMV. Spleen and femurs were harvested 3 and 5 days after infection. As controls, mice were injected with PBS. A) Isolated splenocytes were lineage depleted. CFU-E abundance in the spleen. B) Proliferative state of splenic CFU-E. C) CFU-E abundance in the bone marrow. D) Proliferative state of bone marrow CFU-E. (A-D) n=3-6, N=2. Mean percentages ± SEM are given. Statistical analysis was performed on square root transformed data using a t-test (A and C) and one-way ANOVA with Bonferroni post-hoc test (B and D). p<0.05 is considered as statistically significant; p-values between 0.05 and 0.1 are indicated (statistical significance between the genotypes). n, biological replicates; N, experimental repetitions.*

### 4.2 The absence of STAT1 signaling in myeloid cells increases the frequency of splenic, but not bone marrow MkP, during MCMV infection

Our group has established that upon infection with MCMV, *Stat1*$^{\Delta M/PMN}$ mice exhibit impaired extramedullary megakaryopoiesis, as evidenced by decreased splenic MK numbers and lower platelet counts in the blood (Gawish et al. 2019). We wanted to investigate whether differences between infected *Stat1*$^{\Delta M/PMN}$ and *Stat1*$^{fl/fl}$ mice already occur at the stage of MkP. Thus, we used flow cytometry to assess the abundance and proliferative state of MkP in the spleen and bone marrow of *Stat1*$^{\Delta M/PMN}$ and *Stat1*$^{fl/fl}$ mice.

Upon infection, MkP were detectable in the spleens of *Stat1*$^{\Delta M/PMN}$ mice and littermate controls, thus indicating that both genotypes are able to induce MCMV-triggered extramedullary megakaryopoiesis (Fig. 8A). We found significantly higher amounts of splenic MkP in *Stat1*$^{\Delta M/PMN}$ mice when compared to the controls at both time points p.i. (Fig. 8A). At day 3 p.i., the S phase population was significantly higher in *Stat1*$^{\Delta M/PMN}$ compared to *Stat1*$^{fl/fl}$ mice, indicating a higher proliferative rate (Fig. 8B). At day 5 p.i. *Stat1*$^{\Delta M/PMN}$ and *Stat1*$^{fl/fl}$ mice showed no differences in the cell cycle distribution (Fig. 8B).

MCMV infection did not affect the abundance of bone marrow MkP and no differences were detected between *Stat1*$^{\Delta M/PMN}$ and littermate controls (Fig. 8C). The majority of bone marrow MkP were in the G0-G1 and S phase of the cell cycle and no differences were detected between mice of the two genotypes in any of the experimental conditions (Fig. 8D).

Collectively, these results suggest that during MCMV infection, the absence of myeloid STAT1 causes an increase appearance of MkP, which is associated with a slightly enhanced proliferation, in spleen but not bone marrow .

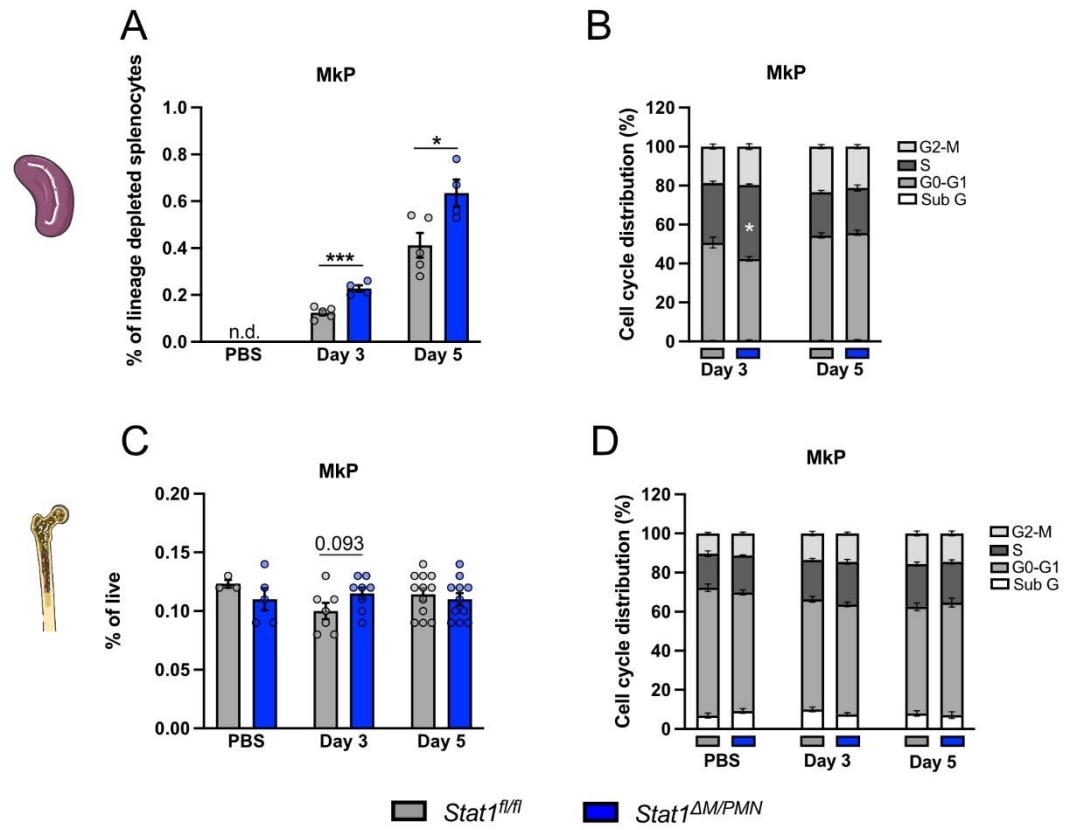


*Figure 8: Absence of STAT1 signalling in myeloid cells results in higher splenic MkP numbers and increased proliferation rate of MkP during early MCMV infection, while bone marrow MkP are not affected. Mice were infected with 5 x $10^4$ PFU/mL of SG-MCMV. Spleen and femurs were harvested 3 and 5 days after infection. As controls, mice were injected with PBS. A) Isolated splenocytes were lineage depleted. MkP abundance in the spleen. B) Proliferative state of splenic MkP. C) MkP abundance in the bone marrow. D) Proliferative state of bone marrow MkP. (A-D) n=3-6, N=2 (N=1 for PBS controls). Mean percentages ± SEM are given. Statistical analysis was performed on square root transformed data using a t-test (A and C) and one-way ANOVA with Bonferroni post-hoc test (B and D). p<0.05 is considered as statistically significant; *p ≤ 0.05, ***p ≤ 0.001; p-values between 0.05 and 0.1 are indicated (statistical significance between the genotypes). n, biological replicates; N, experimental repetitions.*

### 4.3 Absence of STAT1 in myeloid cells alters the cytokine milieu in the spleen during MCMV infection

Next, we wanted to investigate whether differences in EMH between *Stat1*$^{\Delta M/PMN}$ and *Stat1*$^{fl/fl}$ mice correlate with differences in the levels of cytokines and chemokines involved in haemeotopoiesis.

As expected, we observed elevated concentrations of IFNγ and IL-6 in both genotypes upon MCMV infection (Fig. 9A-B). At day 3 p.i. the concentrations of IFNγ as well as IL-6 were significantly higher in *Stat1*$^{\Delta M/PMN}$ mice when compared to controls (Fig. 9A-B). At day 5 p.i. IFNγ and IL-6 concentrations return to basal values, with no differences between the genotypes. MCMV infection induced a downregulation of IL-11 in both genotypes, which was more pronounced on day 3 p.i. in *Stat1*$^{\Delta M/PMN}$ than *Stat1*$^{fl/fl}$ mice (Fig. 9C). LIF was transiently upregulated with no differences between mice of the two genotypes (Fig. 9D). GM-CSF was induced by the infection and slightly higher in *Stat1*$^{\Delta M/PMN}$ compared to *Stat1*$^{fl/fl}$ mice at day 3 p.i. (Fig. 9E). At day 5 p.i. GM-CSF was undetectable in mice of both genotypes (Fig. 9E). SCF was significanty increased at day 3 p.i. and significantly decreased on day 5 p.i. in *Stat1*$^{\Delta M/PMN}$ mice compared to *Stat1*$^{fl/fl}$ mice (Fig. 9F). EPO concentrations in the spleen did not change during MCMV infection and were comparable between mice of the two genotypes (Fig. 9G). CXCL12 levels decreased in *Stat1*$^{\Delta M/PMN}$ and *Stat1*$^{fl/fl}$ mice in response to MCMV infection, with no differences between the genotypes (Fig. 9H). TPO and IL-3 were not detectable.

Taken together, our results suggest that the absence of STAT1 in myeloid cells results in an increased MCMV-induced upregulation of IFNγ, IL-6, GM-CSF and SCF and a slightly stronger downregulation of IL-11 in the spleen.

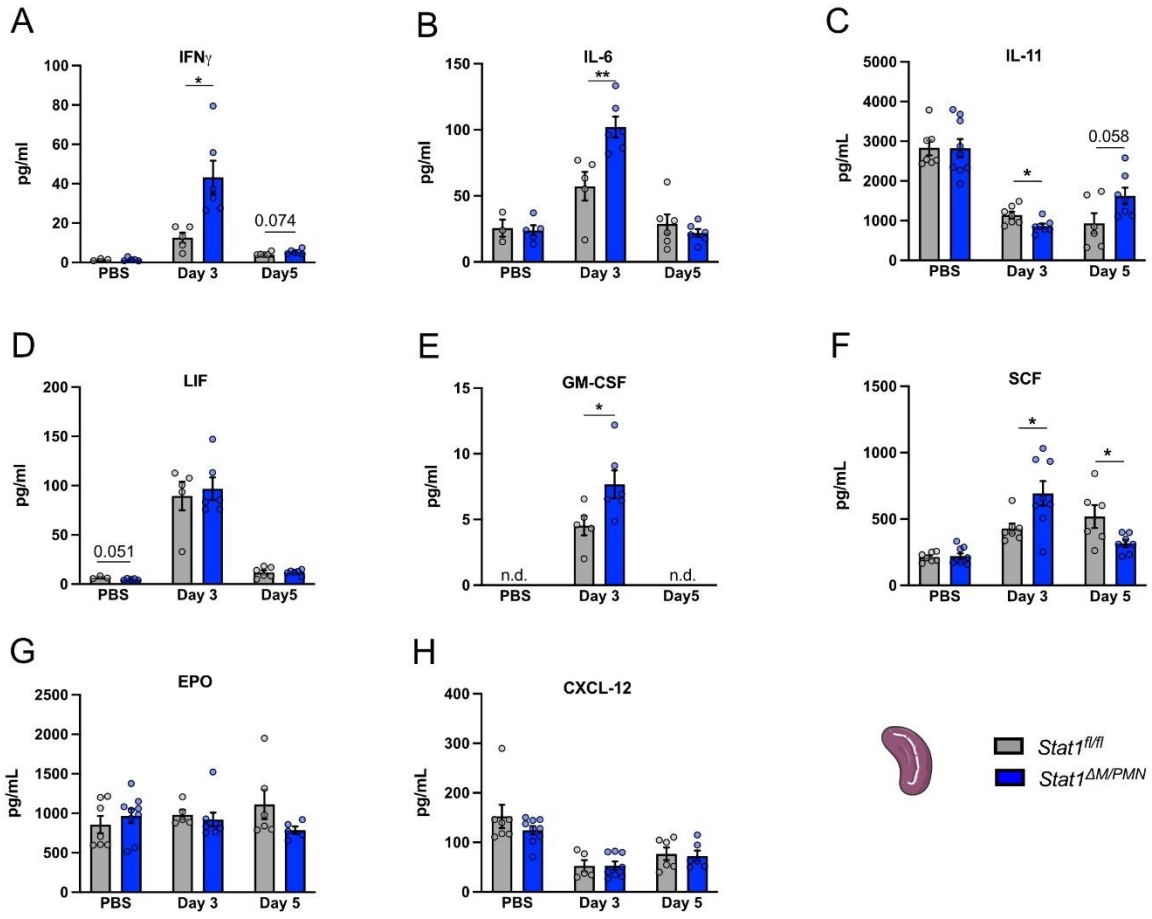


*Figure 9: STAT1 signaling in myeloid cells regulates IFNγ, IL-6, IL-11, GM-CSF and SCF levels in the spleen in response to MCMV infection. Mice were infected with 5 x $10^4$ PFU/mL of SG-MCMV. Spleens were harvested 3 and 5 days after infection. As controls, mice were injected with PBS. Concertation of A) interferon γ (IFNγ), B) Interleukin – 6 (IL-6), C) Interleukin - 11 (IL-11), D) leukemia inhibitory factor (LIF), E) granulocyte-macrophage colony-stimulating factor (GM-CSF), F) stem cell factor (SCF), G) erythropoietin (EPO), H) C-X-C motif chemokine 12 (CXCL12) in spleen homogenate measured in time indicated. (A-H) n=3-6, N=1-2. Statistical analysis was performed using a t-test. p<0.05 is considered as statistically significant; *p ≤ 0.05, **p ≤ 0.01; p-values between 0.05 and 0.1 are indicated (statistical significance between the genotypes). n, biological replicates; N, experimental repetitions.*

## 5. Discussion

Absence of myeloid STAT1 results in decreased megakaryocyte and erythroblast numbers in the spleen, indicating that STAT1 signalling in myeloid cells promotes extramedullry erythropoiesis and megakaryopoiesis (Gawish et al. 2019). However, the underlying mechanisms remain elusive. In the present study, we assessed the abundance and the proliferative state of MkP and CFU-E in the spleen of MCMV-infected *Stat1*$^{\Delta M/PMN}$ mice and littermate controls and measured cytokines and chemokines involved in haematopoiesis. In parallel, the abundance and proliferative state of MkP and CFU-E in the bone marrow were assessed to investigate whether or not splenic haematopoiesis mirrors haematopoietic responses in the bone marrow.
We show here, that during MCMV infection the absence of STAT1 signaling in myeloid cells results in an increased frequency of MkP in the spleen, but not in the bone marrow, while it does not affect splenic and bone marrow CFU-E numbers.

Previous studies in our laboratory have shown significantly lower MKs in MCMV infected *Stat1*$^{\Delta M/PMN}$ mice when compared to *Stat1*$^{fl/fl}$ mice (Gawish et al. 2019). Surprisingly, we found that the number of MkP, the immediate precursors of MKs, is significantly higher in *Stat1*$^{\Delta M/PMN}$ mice at both time points p.i. as compared to littermate controls. These results suggest that MkP fail to differentiate into MK when myeloid STAT1 is missing. Alternatively, but not mutually exclusively, the increased MkP frequency could be due to the slightly higher proliferative rate of *Stat1*$^{\Delta M/PMN}$ MkP compared to controls observed in our experiments. As components of the haematopoietic niche, macrophages participate in shaping the local cytokine milieu by responding to environmental signals and consequently impact megakaryopoiesis (D'Atri et al. 2011, Zhao et al. 2021). In our study, we found significantly increased concentrations of IL-6, GM-CSF and SCF in the spleens of *Stat1*$^{\Delta M/PMN}$ mice compared to the littermate controls. These cytokines have been reported to enhance MkP proliferation in presence of IL-3 and TPO (Metcalf et al. 2002, Yu and Cantor 2012). However, we were unable to detect TPO and IL-3 in spleen homogenates at day 3 and day 5 p.i. and in PBS controls. TPO is the main driver of MkP proliferation and differentiation (Kaushansky et al. 1994) and is primarily produced by the liver (Hitchcock and Kaushansky 2014). Thus, it would be important to also measure TPO levels in the peripheral blood. There is increasing evidence that during inflammation macrophages secrete cytokines that can suppress MkP proliferation, such as IL-8 and TNFα (D'Atri et al. 2011, Zhao et al. 2021, Adeli et al. 2011, Jiang et al. 2022, Lu et al. 2000). It is

thus possible that absence of STAT1 signaling in myeloid cells relieves an inhibitory interaction between macrophages and MkP, albeit this clearly needs further investigation.
Another important finding of our study is that there was no difference in MkP abundance in the bone marrow between mice of the two genotypes, indicating that the impact of STAT1 signalling in myeloid cells on megakaryopoiesis is spleen-specific.

Mice lacking STAT1 in myeloid cells have decreased numbers of erythroblasts in the spleen after MCMV infection compared to littermate controls (Gawish et al. 2019). We show here that the abundance of their immediate precursors, CFU-E, is not affected by the absence of STAT1 in myeloid cells, suggesting that STAT1 signalling in myeloid cells promotes the differentiation of CFU-E into erythroblasts. We found no difference in the concentrations of EPO, a major driver of erythropoiesis, in the spleens of *Stat1*$^{\Delta M/PMN}$ and *Stat1*$^{fl/fl}$ mice, suggesting that the phenotype of *Stat1*$^{\Delta M/PMN}$ is independent of EPO. CFU-E are the first erythroid progenitors to adhere to the central macrophage in EBIs (Sadahira and Mori 1999) and lack of direct interaction between late stage CFU-E and the macrophage results in decreased erythroblast numbers (Rhodes et al. 2008). Thus, it is possible that the absence of STAT1 signalling in myeloid cells, including macrophages, results in problems with the adherence of either CFU-E or erythroblasts to the central macrophage. Alternatively, lower erythroblast numbers in *Stat1*$^{\Delta M/PMN}$ mice could be associated with decreased erythroblast survival or decreased proliferation, which needs further examination. There is evidence that macrophage-expressed adhesion molecules, such as erythroblast macrophage protein (Emp), intracellular adhesion molecule 4 (ICAM4) and VCAM-1, are required for EBI-associated erythroblast survival and maturation (Hanspal et al.1998, Soni et al. 2006, Wei et al. 2019). Erythroblasts in *Stat1*$^{\Delta M/PMN}$ have a more immature phenotype than those in *Stat1*$^{fl/fl}$ mice (Gawish et al. 2019), which is consistent with defects in EBI formation (Hanspal et al.1998, Wei et al. 2019, Wang et al. 2013). STAT1 is capable of inducing the expression of adhesion molecules, including ICAM-1 and VCAM-1 (Jaruga et al. 2004). In future studies, cell surface proteomics could be used to assess the expression of adhesion molecules on splenic macrophages from MCMV infected *Stat1*$^{\Delta M/PMN}$ and *Stat1*$^{fl/fl}$. Furthermore, RNA sequencing of these macrophages may provide further insights.

Collectively, our data suggest that the reduced splenic megakaryopoiesis and erythropoiesis in the absence of STAT1 in myeloid cells is not due to an impaired recruitment or development of MkP and CFUE, respectively, during MCMV infection.

## 6. Summary

Extramedullary haematopoiesis (EMH) is the formation of blood cells outside the bone marrow. In adults, EMH compensates for an increased blood cell demand during infection and inflammation, in particular when bone marrow haematopoiesis in suppressed. Signal transducer and activator of transcription 1 (STAT1) is a key transcription factor used by all types of interferons (IFNs). We have shown previously that mice lacking STAT1 in myeloid cells (*Stat1*$^{\Delta M/PMN}$) have impaired EMH upon infection with murine cytomegalovirus (MCMV) and during sterile inflammation, as evidenced by lower numbers of erythroblasts and megakaryocytes in the spleen. To better understand the mechanism, we assessed the abundance and the proliferative state of their immediate precursors, the colony-forming unit erythroid (CFU-E) and megakaryocyte progenitors (MkP), in spleen and bone marrow at day 3 and day 5 post infection. In addition, we measured levels of cytokines and chemokines that are important in haematopoiesis in the spleen. We show that MCMV infection induces the appearance of CFU-E and MkP in spleens, whereas their frequencies in the bone marrow remains unchanged. The abundance and proliferative state of CFU-E was similar between *Stat1*$^{\Delta M/PMN}$ mice and littermate controls (*Stat1*$^{fl/fl}$mice), indicating that STAT1 signaling in myeloid cells affects erythropoiesis at later developmental stages, such as the differentiation of CFU-E into erythroblasts or erythroblast proliferation/survival. In contrast, *Stat1*$^{\Delta M/\text{PMN}}$ mice had an even higher frequency of splenic MkP than littermate controls, which was associated with a slightly increased proliferative rate. Albeit further studies are needed, this may indicate that myeloid cells promote the differentiation of MkP into megakaryocytes through STAT1-dependent mechanisms. In the bone marrow, the frequency and proliferative state of MkP was similar between *Stat1*$^{\Delta M/\text{PMN}}$ and control mice. With respect to cytokines/chemokines, we found increased MCMV-induced upregulation of splenic interleukin-6 (IL-6), granulocyte-macrophage colony-stimulating factor (GM-CSF), IFNγ and stem cell factor (SCF) and increased downregulation of IL-11 in *Stat1*$^{\Delta M/\text{PMN}}$ compared to control mice. Erythropoietin (EPO), C-X-C motif chemokine 12 (CXCL12) and leukemia inhibitory factor (LIF) levels were similar in mice of the two genotypes. Taken together, our data indicate that STAT1 in myeloid cell regulates splenic EMH at multiple levels and support the notion that EMH does not simply mirror haematopoietic responses in the bone marrow.

## 7. Zusammenfassung

Die Blutbildung außerhalb des Knochenmarks wird als extramedulläre Hämatopoese (EMH) bezeichnet. Im adulten Organismus kommt EMH vor, wenn durch Infektionen oder Entzündungen die Blutbildung im Knochenmark nicht ausreichend ist. “Signal transducer and activator of transcription 1” (STAT1) ist ein wichtiger Transkriptionsfaktor, der von allen Typen an Interferonen (IFN) benutzt wird. Studien aus unserem Labor zeigten, dass Mäuse, denen STAT1 in myeloiden Zellen fehlt (*Stat1*$^{\Delta M/PMN}$ Mäuse), nach Infektion mit dem murinen Cytomegalovirus (MCMV) und während steriler Entzündung, mangelhafte EMH mit einer stark reduzierten Anzahl an Erythroblasten und Megakaryozyten in der Milz aufweisen. Um den Mechanismus besser zu verstehen, haben wir die Anzahl und Proliferation der unmittelbaren Vorläufer von Erythroblasten und Megakaryozyten, den CFU-E und MkP, in der Milz und dem Knochenmark am Tag 3 und 5 nach der MCMV Infektion bestimmt. Zusätzlich wurden Zytokine und Chemokine, die Hämatopoese regulieren können, in der Milz gemessen. Wir konnten zeigen, dass MCMV Infektion das Auftreten von CFU-E und MkP in der Milz induziert, während sich deren Anzahl im Knochenmark nicht verändert. Die Anzahl und Proliferation von CFU-E in der Milz von *Stat1*$^{\Delta M/PMN}$ Mäusen war vergleichbar zu Wurfgeschwistern (*Stat1*$^{fl/fl}$ Mäuse), was nahelegt, dass STAT1 in myeloiden Zellen im späteren Verlauf der Erythropoese, z.B. bei der Differenzierung von CFU-E zu Erythroblasten, eine Funktion hat oder das Überleben oder die Vermehrung der Erythroblasten unterstützt. Im Gegensatz dazu, beobachteten wir eine höhere Anzahl und leicht erhöhte Proliferation von MkP in der Milz von *Stat1*$^{\Delta M/PMN}$ Mäusen. Obwohl weitere Experimente von Nöten sind, könnte dies darauf hinweisen, dass myeloide Zellen mittels STAT1 die Differenzierung von MkP in Megakaryozyten fördern. Zwischen *Stat1*$^{\Delta M/PMN}$ und *Stat1*$^{fl/fl}$ Mäusen gab es keinen Unterschied in der Anzahl und Proliferation von MkP im Knochenmark. In der Milz fanden wir erhöhte Konzentrationen an Interleukin-6 (IL-6), Granulozyten-Makrophagen-Kolonie-stimulierenden Faktor (GM-CSF), IFN$\gamma$ und Stammzellfaktor (SCF) und erniedrigte Konzentrationen an IL-11 in MCMV-infizierten *Stat1*$^{\Delta M/PMN}$ Mäusen im Vergleich zu Kontrollen. Die Mengen an Erythropoetin (EPO), C-X-C-Motiv-Chemokin 12 (CXCL12), und Leukämiehemmendem Faktor (LIF) waren ähnlich in Milzen von Mäusen beider Gentoypen. Zusammenfassend zeigen unsere Daten, dass STAT1 in myeloiden Zellen EMH in der Milz auf verschiedenen Ebenen reguliert und dass EMH nicht einfach nur infektionsinduzierte Haematopoiese im Knochenmark widerspiegelt.

## 8. Abbreviations

**ANOVA** analysis of variance

**BCA** bicinchoninic acid

**BFU-E** burst-forming unit-erythroid

**BMEC** bone marrow endothelial cell

**BMP4** bone morphogenic protein 4

**BSA** bovine serum albumin

**CFU-E** colony-forming unit-erythroid

**CMP** common myeloid progenitor

**CXCL12** CXC-motif-chemokine 12

**DC** dendritic cell

**EBI** erythroblastic island

**EC** endothelial cell

**EMH** extramedullary haematopoiesis

**Emp** erythroblast macrophage protein

**EPO** erythropoietin

**EPOR** erythropoietin receptor

**FELASA** Federation of European Laboratory Animal Science Associations

**FGF4** fibroblast growth factor 4

**GAF** gamma-interferon activated factor

**GAS** gamma activated sequence

**G-CSF** granulocyte-colony stimulating factor

**GM-CSF** granulocyte-macrophage colony-stimulating factor

**GMP** granulocyte/macrophage progenitor

| | |
|---|---|
| **HCMV** | human cytomegalovirus |
| **HSC** | hematopoietic stem cells |
| **HSPC** | hematopoietic stem and progenitor cell |
| **ICAM-1** | intracellular adhesion molecule 1 |
| **ICAM4** | intracellular adhesion molecule 4 |
| **IFN** | interferon |
| **IFNAR** | type I interferon receptor |
| **IFNGR** | interferon γ receptor |
| **IL** | interleukin |
| **IRF9** | interferon regulatory factor 9 |
| **ISG** | interferon stimulated genes |
| **ISGF3** | interferon-stimulated gene factor 3 |
| **ISRE** | interferon-stimulated response element |
| **IT-HSC** | intermediate-term haematopoietic stem cell |
| **JAK** | Janus kinase |
| **LIF** | leukemia inhibitory factor |
| **LIP-CLOD** | liposomal-encapsulated clodronate |
| **LMPP** | lymphoid multipotent progenitor |
| **LPS** | lipopolysaccharide |
| **LT-HSC** | long-term haematopoietic stem cell |
| **MCMV** | murine cytomegalovirus |
| **M-CSF** | macrophage-colony stimulating factor |
| **MEP** | megakaryocyte/erythrocyte progenitor |
| **MK** | megakaryocyte |

| | |
|---|---|
| **MkP** | megakaryocyte progenitor |
| **MPP** | multipotent progenitor |
| **NK cell** | natural killer cell |
| **NLR** | NOD-like receptor |
| **PAMP** | pathogen-associated molecular pattern |
| **PRR** | pattern recognition receptor |
| **RBC** | red blood cell |
| **RPM** | red pulp macrophage |
| **SCF** | stem cell factor |
| **SG-MCMV** | salivary gland-derived murine cytomegalovirus |
| **SH2** | Src-homology 2 |
| **STAT** | signal transducer and activator of transcription |
| **ST-HSC** | short-term haematopoietic stem cell |
| **Tcf21** | transcription factor 21 |
| **TLR** | Toll-like receptor |
| **Tlx1** | T cell leukemia homeobox 1 |
| **TNFα** | tumour necrosis factor α |
| **TPO** | thrombopoietin |
| **TYK2** | tyrosine kinase 2 |
| **Tyr** | tyrosine |
| **VCAM-1** | vascular adhesion molecule 1 |
| **WR** | working reagent |

## 9. Tables and Figures

### Tables



### Figures

## 10. Literature


Aaronson DS, and Horvath CM. 2002. A Road Map for Those Who Don't Know JAK-STAT. *Science,* 296 (5573): 1653–55.

Adeli EK, Abolghasemi H, Ebtekar M, Pourpak Z, and Kheirandish M. 2011. Effects of CXCR1 and CXCR2 Inhibition on Expansion and Differentiation of Umbilical Cord Blood CD133+ Cells into Megakaryocyte Progenitor Cells. *Cytokine,* 55 (2): 181–87.

Akashi K, Traver D, Miyamoto T, and Weissman IL. 2000. A Clonogenic Common Myeloid Progenitor That Gives Rise to All Myeloid Lineages. *Nature,* 404 (6774): 193–97.

Al Sayed MF, Amrein MA, Buhrer ED, Huguenin AL, Radpour R, Riether C, and Ochsenbein AF. 2019. T-Cell–Secreted TNFa Induces Emergency Myelopoiesis and Myeloid-Derived Suppressor Cell Differentiation in Cancer. *Cancer Research,* 79 (2): 346–59.

Alliot C, Beets C, Besson M, and Derolland P. 2001. Spontaneous Splenic Rupture Associated with CMV Infection: Report of a Case and Review. *Scandinavian Journal of Infectious Diseases,* 33 (11): 875–77.

Alves-Rosa F, Vermeulen M, Cabrera J, Stanganelli C, Capozzo A, Narbaitz M, Van Rooijen N, Palermo M, and Isturiz MA. 2003. Macrophage Depletion Following Liposomal-Encapsulated Clodronate (LIP-CLOD) Injection Enhances Megakaryocytopoietic and Thrombopoietic Activities in Mice. *British Journal of Haematology,* 121 (1): 130–38.

Au-Yeung N, Mandhana R, and Horvath CM. 2013. Transcriptional Regulation by STAT1 and STAT2 in the Interferon JAK-STAT Pathway. *Jak-Stat* 2, (3): e23931.

Avecilla ST, Hattori K, Heissig B, Tejada, Liao F, Shido K, Jin DK. 2004. Chemokine-Mediated Interaction of Hematopoietic Progenitors with the Bone Marrow Vascular Niche Is Required for Thrombopoiesis. *Nature Medicine,* 10 (1): 64–71.

Baldridge MT, King KY, Boles NC, Weksberg DC, Goodell MA. 2010. Quiescent Haematopoietic Stem Cells Are Activated by IFN-γ in Response to Chronic Infection. *Nature,* 465 (7299): 793–97.

Bao EL, Cheng AN, and Sankaran VG. 2019. The Genetics of Human Hematopoiesis and Its Disruption in Disease. *EMBO Molecular Medicine,* 11 (8): 1–13.

Belyaev NN, Biró J, Langhorne J, and Potocnik AJ. 2013. Extramedullary Myelopoiesis in Malaria Depends on Mobilization of Myeloid-Restricted Progenitors by IFN-γ Induced Chemokines. *PLoS Pathogens,* 9 (6).

Boettcher S, and Manz MG. 2017. Regulation of Inflammation- and Infection-Driven Hematopoiesis. *Trends in Immunology,* 38 (5): 345–57.

Boisson-Dupuis S, Kong XF, Okada S, Cypowyj S, Puel A, Abel L, and Laurent Casanova J. 2012. Inborn Errors of Human STAT1: Allelic Heterogeneity Governs the Diversity of Immunological and Infectious Phenotypes. *Current Opinion in Immunology,* 24 (4): 364–78.

Bromberg JF, Horvath CM, Wen Z, Schreiber RD, and Darnell JE. 1996. Transcriptionally Active Stat1 Is Required for the Antiproliferative Effects of Both Interferon α and Interferon γ. *Proceedings of the National Academy of Sciences of the United States of America,* 93 (15): 7673–78.

Chasis JA, and Mohandas N. 2008. Erythroblastic Islands: Niches for Erythropoiesis. *Blood,* 112 (3): 470–78.

Chavakis T, Mitroulis I, and Hajishengallis G. 2019. Hematopoietic Progenitor Cells as Integrative Hubs for Adaptation to and Fine-Tuning of Inflammation. *Nature Immunology,* 20 (7): 802–11.

Chen Q, Solar G, Eaton DL, and Sauvage FJ. 1998. IL-3 Does Not Contribute to Platelet Production in c-Mpl-Deficient Mice. *Stem Cells,* 16 Suppl 2: 31–36.

Chiu SC, Liu HH, Chen CL, Chen PR, Liu MC, Lin SZ, and Chang KT. 2015. Extramedullary Hematopoiesis (EMH) in Laboratory Animals: Offering an Insight into Stem Cell Research. *Cell Transplantation,* 24 (3): 349–66.

Chow A, Huggins M, Jalal A, Hashimoto D, Lucas D, Kunisaki Y, Pinho S. 2013. CD169 + Macrophages Provide a Niche Promoting Erythropoiesis under Homeostasis and Stress. *Nature Medicine,* 19 (4): 429–36.

D'Atri LP, Pozner RG, Nahmod KA, Landoni VI, Isturiz M, Negrotto S, and Schattner M. 2011. Paracrine Regulation of Megakaryo/Thrombopoiesis by Macrophages. *Experimental Hematology,* 39 (7): 763–72.

Darnell JE, Kerr IM, and Stark GR. 1994. Jak-STAT Pathways and Transcriptional Activation in Response to IFNs and Other Extracellular Signaling Proteins. *Advancement Of Science,* 264 (5164): 1415–21.

De Bruin AM, Libregts SF, Valkhof M, Boon L, Touw IP, and Nolte MA. 2012. IFNγ Induces Monopoiesis and Inhibits Neutrophil Development during Inflammation. *Blood,* 119 (6): 1543–54.

Decker M, Leslie J, Liu Q, and Ding L. 2018. Hepatic Thrombopoietin Is Required for Bone Marrow Hematopoietic Stem Cell Maintenance. *Science,* 360 (6384): 106–10.

Decker T, Stockinger S, Karaghiosoff M, Müller M, and Kovarik P. 2002. IFNs and STATs in Innate Immunity to Microorganisms. *Journal of Clinical Investigation,* 109 (10): 1271–77.

Dimberg A, Karlberg I, Nilsson K, and Öberg F. 2003. Ser727/Tyr701-Phosphorylated Stat1 Is Required for the Regulation of c-Myc, Cyclins, and P27Kip1 Associated with ATRA-Induced G0/G1 Arrest of U-937 Cells. *Blood,* 102 (1): 254–61.

Dutta P, Hoyer FF, Grigoryeva LS, Sager HB, Leuschner F, Courties G, Borodovsky A. 2015. Macrophages Retain Hematopoietic Stem Cells in the Spleen via VCAM-1. *The Journal of Experimental Medicine*, 212 (4): 497–512.

Essers MAG, Offner S, Blanco-Bose WE, Waibler Z, Kalinke U, Duchosal MA, and Trumpp A. 2009. IFNα Activates Dormant Haematopoietic Stem Cells in Vivo. *Nature,* 458 (7240): 904–8.

Gainsford T, Nandurkar M, Metcalf D, Robb L, Begley GC, and Warren Sa. 2000. The Residual Megakaryocyte and Platelet Production in C-Mpl-Deficient Mice Is Not Dependent on the Actions of Interleukin-6, Interleukin-11, or Leukemia Inhibitory Factor. *Blood,* 95 (2): 528–34.

Gavrilescu LC, Butcher BA, Del Rio L, Taylor GA, and Denkers EY. 2004. STAT1 Is Essential for Antimicrobial Effector Function but Dispensable for Gamma Interferon Production during Toxoplasma Gondii Infection. *Infection and Immunity,* 72 (3): 1257–

64.

Gawish R, Bulat T, Biaggio M, Lassnig C, Bago-Horvath Z, Macho-Maschler S, Poelzl A. 2019. Myeloid Cells Restrict MCMV and Drive Stress-Induced Extramedullary Hematopoiesis through STAT1. *Cell Reports,* 26 (9): 2394-2406.e5.

Gil MP, Bohn E, O'Guin AK, Ramana CV, Levine B, Stark GR, Virgin HW, and Schreiber RD. 2001. Biologic Consequences of Stat1-Independent IFN Signaling. *Proceedings of the National Academy of Sciences of the United States of America,* 98 (12): 6680–85.

Hanspal M, Smockova Y, and Uong Q. 1998. Molecular Identification and Functional Characterization of a Novel Protein That Mediates the Attachment of Erythroblasts to Macrophages. *Blood,* 92 (8): 2940–50.

Hattangadi SM, Wong P, Zhang L, Flygare J, and Lodish HF. 2011. From Stem Cell to Red Cell: Regulation of Erythropoiesis at Multiple Levels by Multiple Proteins, RNAs, and Chromatin Modifications. *Blood,* 118 (24): 6258–68.

Hitchcock IS, and Kaushansky K. 2014. Thrombopoietin from Beginning to End. *British Journal of Haematology,* 165 (2): 259–68.

Hormaechea-Agulla D, Le DT, and King KY. 2020. Common Sources of Inflammation and Their Impact on Hematopoietic Stem Cell Biology. *Current Stem Cell Reports,* 6 (3): 96–107.

Huang S, Bucana CD, Van Arsdall M, and Fidler IJ. 2002. Stat1 Negatively Regulates Angiogenesis, Tumorigenicity and Metastasis of Tumor Cells. *Oncogene,* 21 (16): 2504–12.

Inra CN, Zhou BO, Acar M, Murphy MM, Richardson J, Zhao Z, and Morrison SJ. 2015. A Perisinusoidal Niche for Extramedullary Haematopoiesis in the Spleen. *Nature,* 527 (7579): 466–71.

Jackson A, Nanton MR, O'Donnell H, Akue AD, and McSorley SJ. 2010. Innate Immune Activation during Salmonella Infection Initiates Extramedullary Erythropoiesis and Splenomegaly. *The Journal of Immunology,* 185 (10): 6198–6204.

Jacobsen RN, Forristal CE, Raggatt LJ, Nowlan B, Barbier V, Kaur S, van Rooijen N, Winkler IG, Pettit AR, and Levesque JP. 2014. Mobilization with Granulocyte Colony-Stimulating Factor Blocks Medullar Erythropoiesis by Depleting F4/80+VCAM1+CD169+ER-HR3+Ly6G+ Erythroid Island Macrophages in the Mouse. *Experimental Hematology,* 42 (7): 547-561.e4.

Jaruga B, Hong F, Kim WH, and Gao B. 2004. IFN-γ/STAT1 Acts as a Proinflammatory Signal in T Cell-Mediated Hepatitis via Induction of Multiple Chemokines and Adhesion Molecules: A Critical Role of IRF-1. *American Journal of Physiology - Gastrointestinal and Liver Physiology,* 287 (5 50-5): 1044–52.

Jiang J, Qin J, Li J, Lin X, Zhang B, Fan Z, He L. 2022. Ricolinostat Promotes the Generation of Megakaryocyte Progenitors from Human Hematopoietic Stem and Progenitor Cells. *Stem Cell Research and Therapy*, 13 (1): 1–16.

Johns JL, and Christopher MM. 2012. Extramedullary Hematopoiesis: A New Look at the Underlying Stem Cell Niche, Theories of Development, and Occurrence in Animals. *Veterinary Pathology,* 49 (3): 508–23.

Johns JL, MacNamara KC, Walker NJ, Winslow GM, and Borjesson DL. 2009. Infection with Anaplasma Phagocytophilum Induces Multilineage Alterations in Hematopoietic Progenitor Cells and Peripheral Blood Cells. *Infection and Immunity,* 77 (9): 4070–80.

Jordan S, Ruzsics Z, Mitrović M, Baranek T, Arapović J, Krmpotić A, Vivier E. 2013. Natural Killer Cells Are Required for Extramedullary Hematopoiesis Following Murine Cytomegalovirus Infection. *Cell Host and Microbe*,13 (5): 535–45.

Kaushansky K, Lok S, Holly RD, Broudy VC, Lin N, Bailey MC, Forstrom JW. 1994. Promotion of Megakaryocyte Progenitor Expansion and Differentiation by the C-Mpl Ligand Thrombopoietin. *Nature,* 369 (6481): 568–71.

Kiel MJ, Yilmaz ÖM, Iwashita T, Yilmaz OH, Terhorst C, and Morrison SJ. 2005. SLAM Family Receptors Distinguish Hematopoietic Stem and Progenitor Cells and Reveal Endothelial Niches for Stem Cells. *Cell,* 121 (7): 1109–21.

Kim CH. 2010. Homeostatic and Pathogenic Extramedullary Hematopoiesis. *Journal of Blood Medicine,.* 13–19.

Kim S, Koga T, Isobe M, Kern BE, Yokochi T, Chin YE, Karsenty G, Taniguchi T, and Takayanagi H. 2003. Stat1 Functions as a Cytoplasmic Attenuator of Runx2 in the Transcriptional Program of Osteoblast Differentiation. *Genes and Development,* 17 (16): 1979–91.

King KY, and Goodell MA. 2011. Inflammatory Modulation of HSCs : Viewing the HSC as a Foundation for the Immune Response. *Nature Publishing Group,* 11 (Box 1): 685–92.

Kotenko SV, Izotova LS, Pollack BP, Mariano TM, Donnelly RJ, Muthukumaran G, Cook JR. 1995. Interaction between the Components of the Interferon γ Receptor Complex. *Journal of Biological Chemistry,* 270 (36): 20915–21.

Kovacic B, Stoiber D, Moriggl R, Weisz E, Ott RG, Kreibich R, Levy DE, Beug H, Freissmuth M, and Sexl V. 2006. STAT1 Acts as a Tumor Promoter for Leukemia Development. *Cancer Cell,* 10 (1): 77–87.

Kovtonyuk LV, Manz MG, and Takizawa H. 2016. Enhanced Thrombopoietin but Not G-CSF Receptor Stimulation Induces Self-Renewing Hematopoietic Stem Cell Divisions in Vivo. *Blood,* 127 (25): 3175–79.

Kumar A, Commane m, Flickinger TW, Horvath CM, and Stark GR. 1997. Defective TNF-α-Induced Apoptosis in STAT1-Null Cells Due to Low Constitutive Levels of Caspases. *Science,* 278 (5343): 1630–32.

Lazear HM, Schoggins JW, and Diamond MS. 2019. Shared and Distinct Functions of Type I and Type III Interferons" *Immunity,* 50 (4): 907–23.

Li J, Williams M, Park H, Bastos H. 2021. STAT1 Is Essential for HSC Function and Maintains MHCII Hi Stem Cells That Resists Myeloablation and Neoplastic Expansion." *Blood*.

Li W, Wang Y, Chen L, and An X. 2019. Erythroblast Island Macrophages: Recent Discovery and Future Perspectives. *Blood Science,* 1 (1): 61–64.

Lu L. 2000. Suppressive Effects of TNF-a, TGF-B1, and Chemokines on Megakaryocytic Colony Formation in CD341 Cells Derived from Umbilical Cord Blood Compared with Mobilized Peripheral Blood and Bone Marrow. Journal of Hematotherapy & Stem cell

research, 9: 204: 1–26.

MacNamara KC, Racine R, Chatterjee M, Borjesson D, and Winslow GM. 2009. Diminished Hematopoietic Activity Associated with Alterations in Innate and Adaptive Immunity in a Mouse Model of Human Monocytic Ehrlichiosis. *Infection and Immunity,* 77 (9): 4061–69.

Marins-Dos-Santos A, de Paula Ayres-Silva J, Antunes D, de Carvalho Moreira CJ, Pelajo-Machado M, Alfaro D, Zapata AG. 2022. Oral Trypanosoma Cruzi Acute Infection in Mice Targets Primary Lymphoid Organs and Triggers Extramedullary Hematopoiesis. *Frontiers in Cellular and Infection Microbiology,* (12): 1–12.

Mebius RE, and Kraal G. 2005. Structure and function of the spleen. *Nature,* (5) : 606–16.

Megías J, Yáñez A, Moriano S, O'Connor JE, Gozalbo D, and Gil ML. 2012. Direct Toll-like Receptor-Mediated Stimulation of Hematopoietic Stem and Progenitor Cells Occurs in Vivo and Promotes Differentiation toward Macrophages. *Stem Cells,* 30 (7): 1486–95.

Meissl K, Macho-Maschler S, Müller M, and Strobl B. 2017. The Good and the Bad Faces of STAT1 in Solid Tumours. *Cytokine,* 89: 12–20.

Meraz MA, White MJ, Sheehan KC, Bach EA, Rodig SJ, Dighe AS, Kaplan DH.1996. Targeted Disruption of the Stat1 Gene in Mice Reveals Unexpected Physiologic Specificity in the JAK-STAT Signaling Pathway. *Cel,l* 84 (3): 431–42.

Metcalf D, Di Rago L, and Mifsud S. 2002. Synergistic and Inhibitory Interactions in the in Vitro Control of Murine Megakaryocyte Colony Formation. *Stem Cells,* 20 (6): 552–60.

Millot S, Andrieu V, Letteron P, Lyoumi S, Hurtado-Nedelec M, Karim Z, Thibaudeau O. 2010. Erythropoietin Stimulates Spleen BMP4-Dependent Stress Erythropoiesis and Partially Corrects Anemia in a Mouse Model of Generalized Inflammation. *Blood,* 116 (26): 6072–81.

Mitroulis I, Kalafati L, Hajishengallis G, and Chavakis T. 2018. Myelopoiesis in the Context of Innate Immunity. *Journal of Innate Immunity,* 10 (5–6): 365–72.

Nagai Y, Garrett KP, Ohta S, Bahrun U, Kouro T, Akira S, Takatsu K, and Kincade PW. 2006. Toll-like Receptors on Hematopoietic Progenitor Cells Stimulate Innate Immune System Replenishment. *Immunity,* 6: 801–12.

Najjar I, and Fagard R. 2010. STAT1 and Pathogens, Not a Friendly Relationship. *Biochimie,* 92 (5): 425–44.

Noetzli LJ, French SL, and Machlus KR. 2019. New Insights into the Differentiation of Megakaryocytes from Hematopoietic Progenitors. *Arteriosclerosis, Thrombosis, and Vascular Biology,* 39 (7): 1288–1300.

Oda A, Tezuka T, Ueno Y, Hosoda S, and Amemiya Y. 2018. Niche-Induced Extramedullary Hematopoiesis in the Spleen Is Regulated by the Transcription Factor Tlx1. *Scientific Reports*, no. November 2017: 1–16.

Perry JM, Harandi OF, and Paulson RF. 2007. BMP4, SCF, and Hypoxia Cooperatively Regulate the Expansion of Murine Stress Erythroid Progenitors. *Blood,* 109 (10): 4494–4502.

Pestka S, Krause CD, and Walter MR. 2004. Interferons, Interferon-like Cytokines, and Their

Receptors. *Immunological Reviews,* 202: 8–32.

Pietras EM, Reynaud D, Kang YA, Carlin D, Calero-Nieto FJ, Leavitt AD, Stuart JA, Göttgens B, and Passegué E. 2015. Functionally Distinct Subsets of Lineage-Biased Multipotent Progenitors Control Blood Production in Normal and Regenerative Conditions. *Cell Stem Cell,* 17 (1): 35–46.

Platanias LC. 2005. Mechanisms of Type-I- and Type-II-Interferon-Mediated Signalling. *Nature Reviews Immunology,* 5 (5): 375–86.

Ramana CV, Chatterjee-Kishore M, Nguyen H, and Stark GR. 2000. Complex Roles of Stat1 in Regulating Gene Expression. *Oncogene,* 19 (21): 2619–27.

Ramos P, Casu C, Gardenghi S, Breda L, Crielaard BJ, Guy E, Marongiu MF. 2013. Macrophages Support Pathological Erythropoiesis in Polycythemia Vera and β-Thalassemia. *Nature Medicine,* 19 (4): 437–45.

Rhodes MM, Kopsombut P, Bondurant MC, Price JO, and Koury MJ. 2008. Adherence to Macrophages in Erythroblastic Islands Enhances Erythroblast Proliferation and Increases Erythrocyte Production by a Different Mechanism than Erythropoietin. *Blood,* 111 (3): 1700–1708.

Rodriguez-Fraticelli A, Wolock SL, Weinreb CS, Panero R, Patel SH, Jankovic M, Sun J, Calogero RA, Klein AM, and Camargo FD. 2018. Clonal Analysis of Lineage Fate in Native Haematopoiesis. *Nature,* 553 (7687): 212–16.

Sadahira Y, and Mori M. 1999. Role of the Macrophage in Erythropoiesis. *Pathology International,* 49 (10): 841–48.

Samuel CE. 2001. Antiviral Actions of Interferons. *Clinical Microbiology Reviews,* 14 (4): 778–809.

Sanjuan-Pla A, Macaulay IC, Jensen CT, Woll PS, Luis TC, Mead A, Moore S. 2013. Platelet-Biased Stem Cells Reside at the Apex of the Haematopoietic Stem-Cell Hierarchy. *Nature,* 502 (7470): 232–36.

Sezaki M, Hayashi Y, Wang Y, Johansson A, Umemoto T, and Takizawa H. 2020. Immuno-Modulation of Hematopoietic Stem and Progenitor Cells in Inflammation. *Frontiers in Immunology,* 11: 1–16.

Sommerkamp P, Romero-Mulero MC, Narr A, Ladel L, Hustin L, Schönberger K, Renders S. 2021. Mouse Multipotent Progenitor 5 Cells Are Located at the Interphase between Hematopoietic Stem and Progenitor Cells. *Blood,* 137 (23): 3218–24.

Stark GR, Cheon H, and Wang Y. 2018. Responses to Cytokines and Interferons That Depend upon JAKs and STATs. *Cold Spring Harbor Perspectives in Biology*,10 (1).

Stephanou A, and Latchman DS. 2005. Opposing Actions of STAT-1 and STAT-3. *Growth Factors,* 23 (3): 177–82.

Sugawara I, Yamada H, and Mizuno S. 2004. STAT1 Knockout Mice Are Highly Susceptible to Pulmonary Mycobacterial Infection. *Tohoku Journal of Experimental Medicine,* 202 (1): 41–50.

Vignali DAA, and Kuchroo VK. 2012. IL-12 Family Cytokines: Immunological Playmakers. *Nature Immunology,* 13 (8): 722–28.

Wallner B, Leitner NR, Vielnascher RM, Kernbauer E, Kolbe T, Karaghiosoff M, Rülicke T, Decker T, and Müller M. 2012. Generation of Mice with a Conditional Stat1 Null Allele. *Transgenic Research,* 21 (1): 217–24.

Wang Z, Vogel O, Kuhn G, Gassmann M, and Vogel J. 2013. Decreased Stability of Erythroblastic Islands in Integrin B3-Deficient Mice. *Physiological Reports,* 1 (2): 1–14.

Wei Q, Boulais PE, Zhang D, Pinho S, Tanaka M, and Frenette PS. 2019. Maea Expressed by Macrophages, but Not Erythroblasts, Maintains Postnatal Murine Bone Marrow Erythroblastic Islands. *Blood,* 133 (11): 1222–32.

Wilson A, and Trumpp A. 2006. Bone-marrow haematopoietic-stem-cell niches. *Nature,* 6: 93–106.

Wu H, Liu X, Jaenisch R, and Lodish HF. 1995. Generation of Committed Erythroid BFU-E and CFU-E Progenitors Does Not Require Erythropoietin or the Erythropoietin Receptor. *Cell,* 83 (1): 59–67.

Yamamoto R, Morita Y, Ooehara J, Hamanaka S, Onodera M, Rudolph KL, Ema H, and Nakauchi H. 2013. Clonal Analysis Unveils Self-Renewing Lineage-Restricted Progenitors Generated Directly from Hematopoietic Stem Cells. *Cell,* 154 (5): 1112–26.

Yu M, and Cantor AB. 2012. Megakaryopoiesis and Thrombopoiesis: An Update on Cytokines and Lineage Surface Markers. *Methods in Molecular Biology,* 788: 291–303.

Zhang Y, Gao S, Xia J, and Liu F. 2018. Hematopoietic Hierarchy – An Updated Roadmap. *Trends in Cell Biology,* 28 (12): 976–86.

Zhao HY, Zhang YY, Xing T, Tang SQ, Wen Q, Shi Lyu Z, Lv M. 2021. M2 Macrophages, but Not M1 Macrophages, Support Megakaryopoiesis by Upregulating PI3K-AKT Pathway Activity. *Signal Transduction and Targeted Therapy*, 6 (1).

Zhao JL, and Baltimore D. 2015. Regulation of Stress-Induced Hematopoiesis. *Current Opinion in Hematology,* 22 (4): 286–92.

Zhao JL, Chao M, O'Connell RM, Mehta A, Diloreto R, Heath JR, and Baltimore D. 2014. Conversion of Danger Signals into Cytokine Signals by Hematopoietic Stem and Progenitor Cells for Regulation of Stress-Induced Hematopoiesis. *Cell Stem Cell*, 14 (4):